# A Survey on Channel Sounding Technologies and Measurements for UAV-Assisted Communications

Kai Mao, *Graduate Student Member, IEEE*, Qiuming Zhu, *Senior Member, IEEE*, Cheng-Xiang Wang, *Fellow, IEEE*, Xuchao Ye, Jorge Gomez-Ponce, *Member, IEEE*, Xuesong Cai, *Senior Member, IEEE*, Yang Miao, *Senior Member, IEEE*, Zhuangzhuang Cui, *Member, IEEE*, Qihui Wu, *Fellow, IEEE*, Wei Fan, *Senior Member, IEEE*

***Abstract*—Unmanned aerial vehicles (UAVs) have been widely used in both military and civilian applications, where a stable communication link is vital for safe flight control and robust data transmission. To develop a reliable UAV communication system, it is necessary to deeply understand the UAV channel characteristics and establish accurate channel models. Channel sounding is the most effective way to obtain realistic channel characteristics and validate the theoretical channel model. However, the studies on UAV channel sounding are still insufficient in terms of system design and data processing due to the complexity of developing a UAV channel sounder. Different from the terrestrial channel sounders, the implementation of a UAV channel sounder is tortured by the limited battery life and payload capacity of the UAV platform. The sounding scheme and data post-processing also need to be specially designed for highly dynamic UAV channels. So far, most existing survey studies on UAV channels focus on modeling methodology and model presentation. To fill this gap, this paper provides a comprehensive survey on the design of the UAV channel sounder, in terms of the hardware scheme, sounding signal, time synchronization, calibration, and data post-processing. Current issues and potential research topics behind existing sounding technologies and measurement campaigns are analyzed. Moreover, future challenges and open issues are also discussed.**

***Index Terms*—Channel sounding, channel sounder, sounding schemes, unmanned aerial vehicle (UAV), UAV propagation channel.**

This work was supported in part by the National Natural Science Foundation of China (No. 62271250), in part by the Key Technologies R&D Program of Jiangsu (Prospective and Key Technologies for Industry) under Grants BE2022067, BE2022067-1, and BE2022067-3, and in part by Natural Science Foundation of Jiangsu Province (No. BK20211182) *(Corresponding author: Q. Zhu and C.-X. Wang.)*

K. Mao is with The Key Laboratory of Dynamic Cognitive System of Electromagnetic Spectrum Space, College of Electronic and Information Engineering, Nanjing University of Aeronautics and Astronautics, Nanjing 211106, China, and is with The Radio Systems, Faculty of Electrical Engineering Computer Science and Mathematics (EEMCS), University of Twente, the Netherlands (e-mail: maokai@nuaa.edu.cn).

Q. Zhu is with The Key Laboratory of Dynamic Cognitive System of Electromagnetic Spectrum Space, College of Electronic and Information Engineering, Nanjing University of Aeronautics and Astronautics, Nanjing 211106, China, and also with the National Mobile Communications Research Laboratory, Southeast University, Nanjing 210096, China (e-mail: zhuqiuming@nuaa.edu.cn).

C.-X. Wang is with the National Mobile Communications Research Laboratory, Southeast University, Nanjing 210096, China, and also with the Purple Mountain Laboratories, Pervasive Communication Research Center, Nanjing 211111, China (e-mail: chxwang@seu.edu.cn).

X. Ye, and Q. Wu are with The Key Laboratory of Dynamic Cognitive System of Electromagnetic Spectrum Space, College of Electronic and Information Engineering, Nanjing University of Aeronautics and Astronautics, Nanjing 211106, China (e-mail: yexuchao@nuaa.edu.cn, wuqihui2014@sina.com).

Jorge Gomez-Ponce is with the Ming Hsieh Department of Electrical and Computer Engineering, University of Southern California, Los Angeles, CA 90089 USA, and also with the Facultad de Ingeniería en Electricidad y Computación, Escuela Superior Politécnica del Litoral (ESPOL), ESPOL Polytechnic University, Guayaquil 090902, Ecuador (e-mail: gomezpon@usc.edu).

X. Cai is with the Department of Electrical and Information Technology, Lund University, 22100 Lund, Sweden (email: xuesong.cai@eit.lth.se).

Y. Miao is with The Radio Systems, Faculty of Electrical Engineering Computer Science and Mathematics (EEMCS), University of Twente, the Netherlands (e-mail: y.miao@utwente.nl).

Z. Cui is with the WaveCoRE of Department of Electrical Engineering (ESAT), KU Leuven, 3000 Leuven, Belgium (e-mail: zhuangzhuang.cui@kuleuven.be).

W. Fan is with National Mobile Communications Research Laboratory, School of Information Science and Engineering, Southeast University, Nanjing 210096, China (e-mail: weifan@seu.edu.cn).

## I. Introduction

UNMANNED aerial vehicle (UAV) was first invented for the strategic reconnaissance, battlefield surveillance and military attack in the Great War, while the development of commercial UAVs has boosted numerous civilian applications, e.g., precise agriculture, fire monitoring, disaster rescue, product delivery, and so on [1], [2]. According to the report of Allied Market Research, the UAV market is projected to grow from $24.72 billion in 2020 to $70.91 billion by 2030 [3].

Wireless communication has been an indispensable supporter of unmanned aircraft system (UAS). In general, the radio links include the control and non-payload communication (CNPC) link and the payload communication link [4]. The CNPC link is used for the UAV control, which is critical for the safe flight. The payload communication link is used for data transmission, i.e., images, video streams, and other mission-related information. Recently, UAV-assisted communication systems have attracted a lot of interest for potential applications, i.e., aerial base stations (ABSs), flight relays, and cell-free UAV communication networks [5]. In the sixth-generation (6G) communication networks, the UAV communication link is expected to be a bridge connecting the space-air-ground-sea nodes [6], [7]. To ensure the reliable UAV control and robust data transmission, it is necessary to deeply study UAV channels, e.g., air- to-ground (A2G) and air-to-air (A2A) channels, for better designing, optimizing, and evaluating a reliable and robust UAV communication link. For instance, the delay spread of UAV channels is a vital reference for the symbol interval. The duration time of channel fading is important for the interleaving algorithm.

Different from terrestrial mobile channels, UAV channels have some unique features, i.e., three-dimensional (3D) scattering environment, six-dimensional (6D) motion (i.e., 3D trajectory and 3D posture rotation), airframe fading, and so

on [8]–[10]. Therefore, the existing terrestrial channel models cannot be applied to characterize UAV channels directly. Although lots of UAV-related channel models have been proposed in recent years [11]–[14], most of them are not fully validated and testified in various UAV communication scenarios.

To tackle this issue, channel measurements are considered as a valuable means to support the studies and standardize channel models. On the one hand, channel measurement data is fundamental to fit empirical channel models and determine channel model parameters. On the other hand, channel measurement data is the most accurate reference for evaluating the simulation performance of channel models. However, measurement activities for UAV channels are much less than theoretical studies. Firstly, most of UAVs are small aerial platforms with limited capacity and payload. It brings a big challenge to the design of channel sounding hardware. Some large aircraft such as fighter aircraft, airships, and fixed-wing UAVs, are used to carry heavy devices and perform the channel measurements, but they are difficult to popularize due to high costs. Secondly, the channel sounding scheme and data processing algorithm need to be redesigned, since the UAV channels show highly dynamic and non-stationary characteristics. Therefore, it is necessary to investigate and summarize the existing technologies, research gaps, and potential challenges involving the design of UAV channel sounders, in order to help beginners quickly develop a UAV channel sounder and also provide experienced researchers new insights into UAV channel measurements.

Several survey papers involving UAV channels can be found in [13]–[20]. However, all of them mainly focus on the survey of UAV channel modeling methodologies and channel models. Some UAV channel measurement campaigns were mentioned in [13], [14], [16]–[19], but only from the perspective of measurement-based channel modeling. In [14], a table for some UAV channel measurement configurations was provided. However, since channel measurement is not the main focus, these channel measurement configurations were not fully analyzed and did not cover all key aspects of the UAV channel sounder. To fill this gap, this paper is the first survey aiming at the design of UAV channel sounders, including comprehensive aspects that contains hardware implementation, scheme design, and signal processing. Note that this survey is based on numerous literature related to UAV, drone, aerial, A2G, A2A channel sounding, measurements, and analysis [21]– [123]. In particular, we summarize key

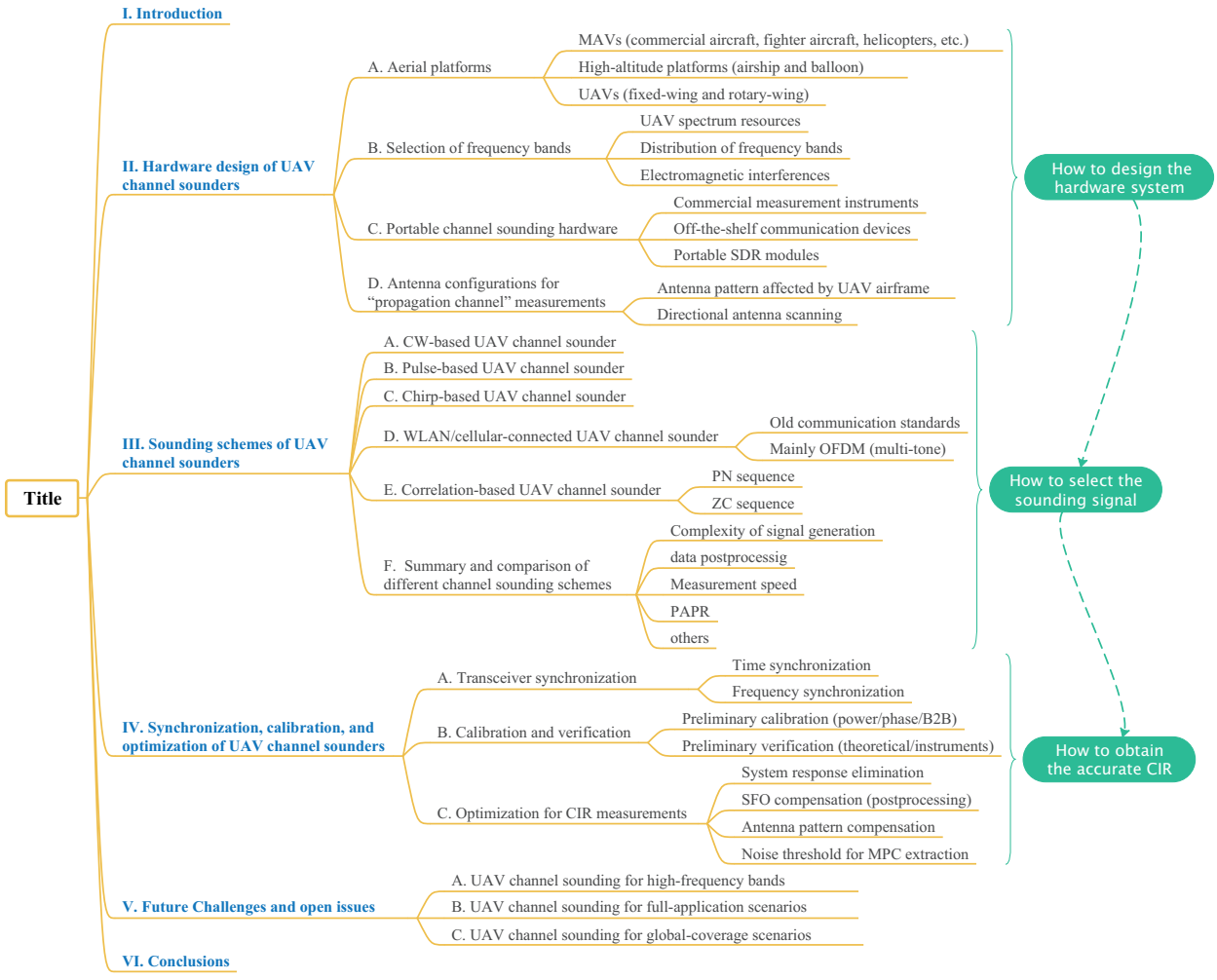


Fig. 1. Mindmap of this paper.

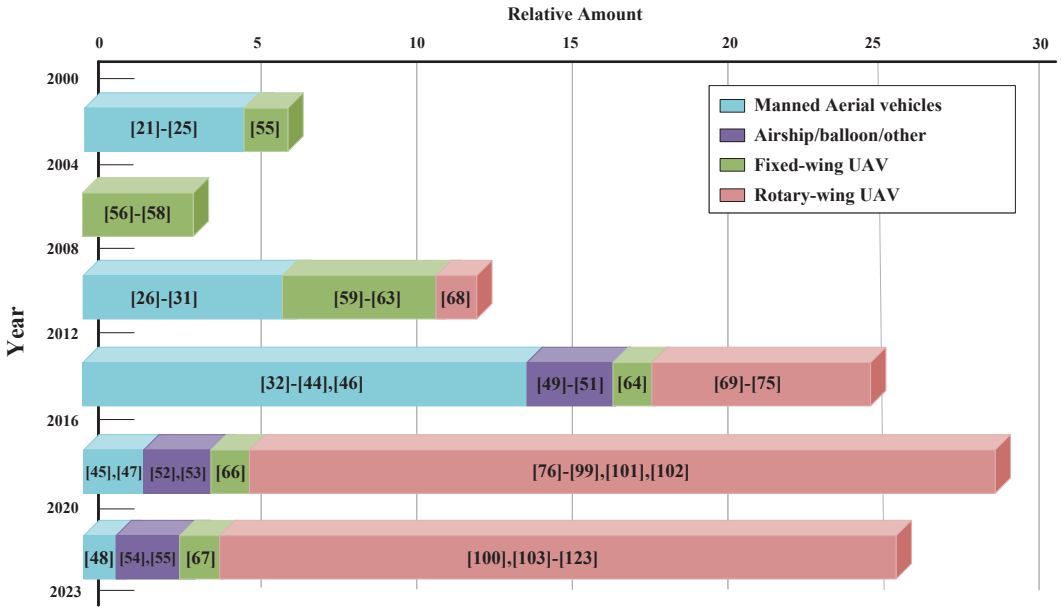


Fig. 2. Evolution timeline of aerial platforms for UAV channel measurements.

issues regarding UAV channel sounding technologies including aerial platform, frequency band, sounding module, antenna configuration, sounding scheme, synchronization, calibration, and optimization. In Table I, we present the configurations of typical UAV channel sounders. The definitions of some abbreviations such as GPS, RSS, RT, etc. can be found at the bottom of Table I.

The rest of this paper is organized as follows. The topics regarding the hardware design of UAV channel sounder are discussed in Section II. In Section III, sounding schemes based on different sounding signals are summarized and compared. In Section IV, issues and possible solutions for synchronization, calibration, and data post-processing of UAV channel sounder are presented. Future challenges and open issues for UAV channel measurements are given in Section V. Finally, conclusions are drawn in Section VI. For the convenience of readers, we provide a navigation figure for the organization of this paper as shown in Fig. 1.

## II. Hardware Design of UAV Channel Sounders

### A. Aerial platforms

UAV channels have some unique features such as six-dimensional (6D) motions and airframe shadowing [10], which requires the aerial platform capable of measuring these features. Moreover, the battery life, load capacity, and accessibility are also important factors. The requirements of aerial platforms for UAV channel measurements are summarized as follows.

• **Battery life and load capacity.** The channel sounder with better performance is usually bigger and heavier. Therefore, the battery life and load capacity of the aerial platform might be crucial factors for the functionality, reliability, and accuracy of UAV channel sounding. Long battery life can also avoid frequent battery replacement and increase the measurement efficiency.

• **Accessibility.** The accessibility of aerial platforms is relative to its price and ease of use. For instance, fixed-wing UAVs and some manned aerial vehicles (MAVs) such as commercial aircraft, fighter aircraft, and helicopters have poor accessibility, since they are generally too costly for most researchers and also difficult to get. Accessibility is the key factor in determining the popularity of aerial platforms.

• **Hovering.** Hovering is a unique flight phase of rotary-wing aerial platforms like helicopters and rotary-wing UAVs (also called drones). In some application scenarios such as disaster areas, an ABS needs to hover over a specific area to provide internet connectivity. There are many UAV channel measurement campaigns performed in a hovering state [99], [115], [121].

• **6D motion.** Unlike terrestrial mobile communication channels, UAV channels have the unique 6D motion characteristic [10], [124]. Therefore, 6D motion is also an essential ability for the aerial platform. Note that some large aircraft (such as commercial passenger aircraft) and high-altitude platforms (such as airships and balloons) cannot perform the sharp 6D motions.

• **Airframe shape.** The airframe shape has been proven to have an impact on the UAV channel characteristics [10], [122]. The airframe might block the propagation path and lead to shadow fading. Moreover, the propagation paths could be reflected or scattered by the airframe. Therefore, the airframe shape of aerial platforms should be similar to those of typical UAV platforms.

The above requirements need to be carefully considered when selecting an aerial platform for carrying a UAV channel sounder hardware. As shown in Fig. 2, we have investigated the existing aerial platforms for UAV channel measurements. The common ones include MAVs [21]–[48], high-altitude platforms [49]–[55], and UAVs (fixed-wing and rotary-wing UAVs) [56]–[123]. Table II presents the comparison of differ-

TABLE I
SUMMARY OF TYPICAL CHANNEL SOUNDERS FOR UAV COMMUNICATIONS.

| Ref. | UAV Platform | Scenario | Aerial Sound. Module | Freq. [GHz] | BW [MHz] | Antenna Setup | Sound. Sig. | Sync. | Cal. & Verif. |
|---|---|---|---|---|---|---|---|---|---|
| [57] | Fixed-wing | A2G (Airfield) | WLAN adapter | 5.28 | - | Aerial: 4 Omni. GS: 2 Omni. | 802.11a | - | - |
| [64] | Fixed-wing | A2G (Farmland) | MID | - | - | Aerial: 4 Omni. GS: 1 Omni. | 802.11b/g | - | - |
| [63] | Quadcopter | A2G (Rural/urban) | - | 0.868/ 2.4 | - | Aerial: 3 Omni. GS: 2 Omni. | 802.11s | - | - |
| [69]–[71] | Quadcopter | A2G (Open field) | WLAN device | 5.24 | 20 | Aerial: 3 Omni. GS: 3 Omni. | 802.11a | Data packet | Throughput |
| [34] | MAV | A2G (Island) | Signal generator | 5.06 | 20 | Aerial: 1 Omni. GS: 1 Omni. | Chirp | GPS/ Rubidium | - |
| [65] | Fixed-wing | A2G | FPGA board | 0.915 | 10 | Aerial: 2 Omni. GS: 8 Omni. | PN | GPS | B2B |
| [72] | Hexacopter | A2A | WLAN adapter | 2.4 | - | Aerial: 2 Omni. GS: 2 Omni. | 802.11n | - | RSS |
| [74] | Quadcopter | A2G (Campus) | P410 UWB | 4.3 | 2200 | Aerial: 1 Omni. GS: 1 Omni. | Pulse | Data packet | - |
| [79], [80] | Quadcopter | A2G (Rural urban) | ISM-band radio | 0.909/ 0.915 | - | Aerial: 1 Omni. GS: 1 Omni. | GSM | - | - |
| [76] | Octocopter | A2G(Desert /residential) | USRP | 5.8 | 20 | Aerial: 1 Omni. GS: 1 Omni. | PN | - | - |
| [81] | Hexacopter | A2G (Factory) | USRP | 2.3/5.8 | 20 | Aerial: 1 Omni. GS: 1 Omni. | OFDM | OFDM packet | VNA and RT |
| [82], [85] | Hexacopter | A2G | TSMA scanner | 0.8 | 20 | Aerial: 1 Omni. | LTE | - | - |
| [83] | Hexacopter | A2G (Suburban) | - | 1.2/4.2 | - | Aerial: 1 Omni. GS: 2 Omni. | CW | - | AC |
| [84] | Quadcopter | A2G (Uma/RMa) | - | 0.919/2.412 | - | Aerial: 2 Omni. GS: 1 Omni. | WLAN/CW | - | 3GPP |
| [66] | Fixed-wing | A2A (Hill/sea) | FPGA board | 5.11 | 7 | Aerial: 1 Omni. GS: 1 Omni. | PN | GPS | - |
| [86] | Quadcopter | A2G (Suburban) | Mobile phone | 0.85 | - | 1 Omni. | LTE | - | - |
| [87] | Hexacopter | A2G | - | 3.9 | 250 | Aerial: 1 Omni. GS: 1 Omni. | Pulse | - | RT |
| [89], [90], [93] | Hexacopter | A2G (suburban) | USRP | 2.585 | 18 | 1 Omni. | LTE | OFDM packet | - |
| [88] | Hexacopter | A2G (Suburban) | USRP | 0.85 | 25 | Aerial: 1 Omni. GS: 1 Omni. | PN | GPS/Disciplined oscillator | - |
| [92] | Quadcopter | A2G (Campus) | FPGA board | 3.5 | 20 | Aerial: 2 Omni. GS: 64 Omni. | PN | GPS | B2B |
| [94], [102] | Hexacopter | A2A | Commercial channel sounder | 5.2 | 100 | Aerial: 1 Omni. Aerial2: 1 Omni. | OFDM | Optical fiber | - |
| [96], [97], [103] | Hexacopter | A2G(Lake /rural/hilly/ (suburban) | DWM1001 UWB | 6.5 | 500 | Aerial: 1 Omni. GS: 1 Omni. | Pulse | - | - |
| [98] | Hexacopter | A2G (UMa) | - | 1/4/12/24 | - | Aerial: 1 Omni. GS: 3 Omni.& 1 Direct | CW | - | - |
| [100] | Hexacopter | A2G (suburban) | USRP | 2.5 | 15.36 | Aerial: 1 Omni. GS: 1 Omni.& 1 Direct | LTE | GPS/Disciplined oscillator | - |
| [95] | Quadcopter | - | USRP | 2.585 | 20 | Aerial: 1 Omni. GS: 1 Omni. | PN | GPS/Disciplined oscillator | B2B |
| [101] | Quadcopter | A2G (Open field) | P440 UWB | 3.95 | 1700 | Aerial: 1 Omni. GS: 2 Omni. | Pulse | Data packet | - |
| [99] | Hexacopter | A2A | Facebook TG radio | 60.48 | 2160 | A1: 288 Omni. A2: 288 Omni. | 802.11a | - | Power |
| [104] | Hexacopter | A2G (Campus) | USRP | 2.4 | 120 | Aerial: 1 Omni. GS: 1 Omni. | ZC | GPS | CE |
| [105], [118] | Hexacopter | A2G (Courtyard) | USRP | 3.5 | 46 | Aerial: 1 Omni. GS: 64 Omni. | OFDM | GPS | B2B |
| [107] | Quadcopter | A2A | USRP | 2.484 | - | Aerial1: 2 Omni. Aerial2: 2 Omni. | CW | - | - |
| [109] | Quadcopter | A2G (Factory) | P410 UWB | 4.2 | 2200 | Aerial: 1 Omni. GS: 1 Omni. | Pulse | - | - |
| [110], [111] | Quadcopter | A2G (Airport) | Spectrum analyzer | 28 | - | Aerial: 1 Omni. GS: 1 Direct. | CW | - | - |
| [114] | Hexacopter | A2G (Playground) | DWM1000 UWB | 5 | 3000 | Aerial: 1 Omni. GS: 5 Omni. | Pulse | - | - |
| [115] | Quadcopter | A2G (Human body) | USRP | 0.9/25 | - | Aerial: 1 Omni. GS: 1 Omni. | CW | - | - |
| [113] | Quadcopter | A2G (suburban) | Smart phone | 3.5 | 100 | Aerial: 1 Omni. | 5G | - | - |
| [67] | Fixed-wing | A2A | USRP | 1.42 | 40 | Aerial1: 1 Omni. Aerial2: 1 Omni. | - | - | RT |
| [116] | Hexacopter | A2G (Hilly) | USRP | 2.585/3.5 | 20 | Aerial: 1 Omni. GS: 1 Omni. | PN | - | B2B |
| [117] | Hexacopter | A2A | BladeRF 2.0 | 5.824 | 8 | Aerial1: 1 Omni. Aerial2: 1 Omni. | Chirp | - | AC |
| [123] | Hexacopter | A2G (Near urban) | FPGA board | 3.5 | 100 | Aerial1: 1 Omni. GS: 4 Omni. | ZC | GPS | CE |

AC: anechoic chamber, B2B: back-to-back, CE: channel emulator, GPS: global positioning system, MID: mobile internet device, OFDM: orthogonal frequency-division multiplexing, PN: pseudo-noise sequence, RSS: received signal strength, RT: ray tracing, SDR: software defined radio, USRP: universal software radio peripheral, UWB: ultra-wideband, ZC: Zadoff-Chu

TABLE II
COMPARISON OF DIFFERENT AERIAL PLATFORMS FOR UAV CHANNEL MEASUREMENTS.

| Aerial platforms | | Battery life | Load capacity | Accessibility | Hovering | 6D motion | Airframe shape |
|---|---|---|---|---|---|---|---|
| MAVs | Commercial | ★★★★ | ★★★★★ | ★ | ★ | ★★★★ | ★★★★ |
| | Fighter | ★★★ | ★★★★ | | | ★★★★★ | |
| | Helicopter | ★★★ | ★★★★ | | ★★★★★ | ★★★★ | |
| Airship/balloon/other | | ★★★★★ | ★★★★ | ★★ | ★★★ | ★★ | ★ |
| Fixed-wing UAV | | ★★ | ★★★ | ★★★ | ★ | ★★★★ | ★★★★★ |
| Rotary-wing UAV | | ★ | ★ | ★★★★★ | ★★★★★ | ★★★★★ | ★★★★★ |
| Note: more ★ means better performance. | | | | | | | |

ent aerial platforms regarding the requirements.

At the early stage, some substitute aerial platforms, such as MAVs (i.e., commercial aircraft, fighter aircraft, helicopter) and high-altitude platforms (i.e., airship and balloon), were used to perform aerial channel measurements. It is because at that time fixed-wing and rotary-wing UAV platforms have not been well popularized and commercialized, and the studies of UAV channels were merely initialized in industry and academia. However, these aerial platforms have some disadvantages when utilized in the UAV channel sounder such as poor accessibility, as shown in Table II. As the safety, stability, and accessibility of rotary-wing UAVs or drones have been greatly improved, it leads to a rapid increase in the use of rotary-wing UAVs for channel measurements since 2016, as shown in Fig. 2. However, the fixed-wing UAV, as a typical UAV type, has been rarely used recently. The main reason is that the rotary UAV has better accessibility, hovering ability, and 6D motion ability than the fixed-wing UAV despite the poor battery life and load capacity. In addition, the rotary-wing UAVs show greater potential advantages in various applications than fixed-wing UAVs, such as agriculture, smart industry, aerial photography, product delivery, and so on. According to the report in [3], the rotary-wing UAV is projected to be the most lucrative type.

Moreover, when selecting an aerial platform, the aviation regulations of different countries or areas are also crucial factors needed to be considered. We present a summary of civil aviation regulations for UAV platforms as shown in Table III. It can be found that most areas limit the flight height and weight of UAVs, which is important for designing UAV

TABLE III
CIVIL AVIATION REGULATIONS FOR UAVS IN SOME COUNTRIES OR AREAS.

| Countries/Areas | Regulator | Height | Weight | Others |
|---|---|---|---|---|
| United Kingdom (UK) | Civil Aviation Authority (CAA) | <120 m | <20 kg | 1) Fly within sight<br>2) Far away from downtown/crowds/airports<br>3) Additional clauses (>7 kg) |
| Germany | Federal Ministry for Transport and Digital Infrastructure (BMVI) | <100 m | – | 1) Fly within sight<br>2) Pilot license (>2 kg)<br>3) Label needed (>0.25 kg) |
| Italy | Italian Civil Aviation Authority | <70 m | – | 1) Fly within sight<br>2) Fly in the daytime |
| Mainland China | Civil Aviation Administration of China (CAAC) | <120 m | – | 1) Fly within sight<br>2) Fly in the daytime<br>3) Real-name registration |
| Hongkong | Civil Aviation Department (CAD) | <30 m | <7 kg | 1) Fly within sight<br>2) Fly in the daytime<br>3) Registration needed (>0.25 kg) |
| Singapore | Civil Aviation Authority of Singapore (CAAS) | <60 m | <7 kg | 1) Fly within sight<br>2) Far away from crowds/airports |
| Korea | Ministry of Land, Infrastructure and Transport (MOLIT) | <150 m | <12 kg | 1) Fly within sight<br>2) Fly in the daytime<br>3) Far away from crowds/airports |
| United States (US) | Federal Aviation Administration (FAA) | <120 m | <25 kg | 1) Fly within sight<br>2) Registration needed (>0.25 kg)<br>3) Far away from crowds/airports |
| Canada | Transport Canada | <122 m | – | 1) Fly within sight<br>2) Fly in the daytime<br>3) 75 m away from vehicles/ships/crowds (1∼ 35 kg)<br>4) 30 m away from vehicles/ships/crowds (0.25∼ 1 kg) |

channel sounders and conducting measurement campaigns. We also need to pay attention to specific weight limitations such as 0.25 kg and 7 kg in case of additional clauses. Moreover, most areas encourage to fly within sight and in the daytime as well as far away from the crowds and airports for security reasons.

### B. Selection of frequency bands

When developing a channel sounder, the frequency band is a fundamental factor for selecting and designing hardware components. With the increasing demand of UAV communications for various applications, some institutions and standard bodies have allocated potential spectrum resources for different UAV communication scenarios [125], [126]. For example, the International Telecommunications Union (ITU) has recommended using 960–977 MHz and 5.03–5.091 GHz for CNPC links. Besides, the frequency band at 900 MHz has been widely utilized for the remote-control link. Recently, 2.4 GHz and 5.8 GHz have become preferable payload frequency bands, due to their high data rate for image sharing, video streaming, and so on. Moreover, UAV is expected to serve as an ABS or flight relay in the 5G communication network, namely 5G-related frequency bands such as 700 MHz, 3300–4200 MHz, 4400–5000 MHz, 24.25–29.5 GHz, 37–40 GHz, etc., are also potential ones for UAV communications [127]. In China, several frequency bands, i.e., 840.5 MHz–845 MHz, 1430 MHz–1444 MHz, and 2408 MHz–2440 MHz are approved for UAV communication links in the line-of-sight (LoS) case [17]. Therefore, the frequency selection for UAV channel sounder should be associated with specific application scenarios at the aforementioned and some other potential frequency bands.

Wireless channel characteristics have been proved to change along with different frequency bands [128]–[130], [132]. Therefore, channel measurements for all the potential frequency bands are worth studying. According to our survey, UAV channel sounders covering many different frequency bands have been developed. Matolak *et al.* in [42]–[45], [47] performed many measurement campaigns that focused on specific frequency bands, i.e., 960-977 MHz and 5.03-5.091 GHz, which provided comprehensive measurement results for understanding the channel characteristics of ITU CNPC link. However, the measurement campaigns at the other frequency bands are less focused. To present the intuitionistic distribution of frequency bands, approximately one hundred pieces of literature involving UAV channel measurement campaigns are summarized, as shown in Fig. 3. Some popular frequency bands, such as 2.4 and 5.8 GHz [72], [76], [84], [104], also gained much attention. Generally, the UAV channel measurements under most frequency bands are still insufficient. In addition, it can be found that UAV channel measurements at millimeter wave (mmWave) bands [98], [99], [110]–[112] are still in their early infancy compared with those at sub-6 GHz bands.

Besides the UAV-related spectrum allocation, some other crucial issues referring to frequency selection also need to be considered. The frequency selection of the channel sounder is usually determined by the target communication system, and the interference issues in the communication system have been addressed. However, the hardware components utilized in the channel sounder could be different from those of practical communication systems, thus the interference issues in the channel sounder also need to be well considered. Firstly, the frequency band of channel measurement should avoid overlapping those of other on-UAV communication links such as the flight control and GPS links, otherwise, the safe flight of UAV is not perfectly guaranteed. Secondly, the electromagnetic interferences to the measured link, including internal and

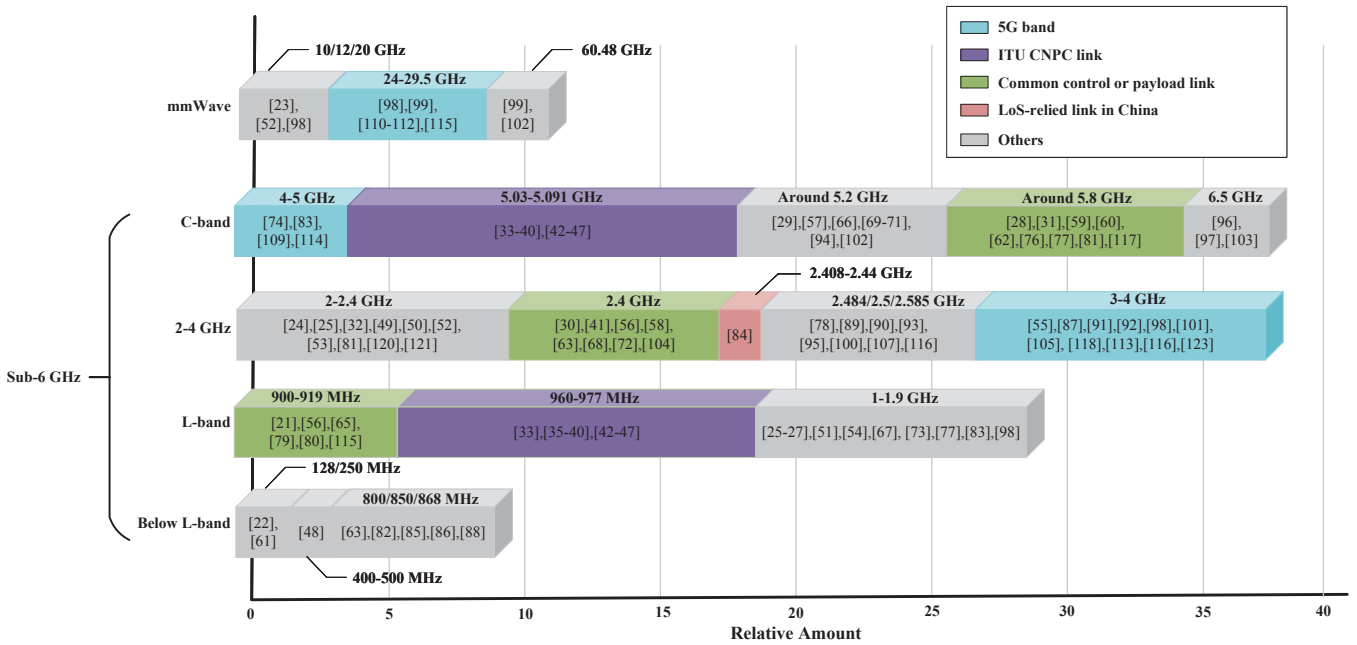


Fig. 3. Frequency bands of existing UAV channel measurement campaigns.

external interferences, are also non-negligible. The internal interferences are usually caused by imperfect electromagnetic compatibility (EMC) of UAV platform, while the external interferences may originate from the other communication systems working at the same frequency bands. In our previous UAV channel measurement campaigns at 3.5 GHz, we found that the measured results could be ruined by interferences, as shown in Fig. 4. Proper frequency bands can be selected to avoid the internal interferences according to the simulated or measured results of UAV EMC [133], [134].

Some fixed external interferences can also be avoided by performing preliminary spectrum occupancy measurements in the target environment [117], [135]. However, unpredictable external interferences at some shared frequency bands might still happen. For example, as an unlicensed frequency band, 2.4 GHz can be used in mobile devices and other unknown WLAN-based communication systems in the environment, which could cause unexpected sporadic interferences during the UAV channel measurement campaigns. On the other hand, we have to utilize specific frequency bands despite external interferences in some applications, such as cellular-connected UAV channel measurements, where the other cellular communication links bring interferences into channel measurement data [137]. In those cases, interference mitigation technology for UAV communications is a possible solution [136], [137]. According to our literature review, no existing work has discussed this issue from the perspective of UAV channel measurements. Therefore, the interference recognition and mitigation of sporadic distorted channel data would be interesting research topics for UAV channel measurements.

Moreover, to obtain complete multi-path information, the UAV channel sounder usually needs to emit the sounding signal with a high transmitting power. In this case, it probably brings a severe interference threat to other communication systems in the environment. When the signal transmitter of channel sounder is placed on the ground or equipped on a UAV at a low altitude, the interference would be easily blocked by surrounding obstacles, so the spread range of interference is limited. However, when the signal transmitter is equipped on a UAV flying at a high altitude of hundreds of meters, the interference signal can propagate over a long distance. Therefore, the interference threat caused by the channel sounder also needs to be carefully considered when selecting the frequency band.

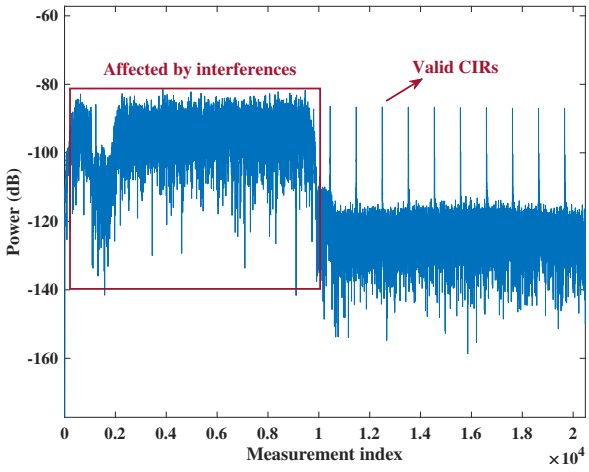


Fig. 4. Measured CIRs affected by interferences.

### C. Portable channel sounding hardware

In Sec. II.A, we find that the rotary-wing UAV platform is widely used for carrying channel sounder hardware. However, the challenge is designing a portable channel sounding hardware that can be mounted on a small UAV platform. According to our survey of UAV channel sounders, the existing channel sounding hardware includes commercial measurement instruments, off-the-shelf communication devices, and SDR modules.

*1) Commercial measurement instruments:*

There are some commercial channel sounders, i.e., MEDAV RUSK [138], Elektrobit PropSound [139], Keysight channel sounder [140], etc. They are designed for terrestrial communication channels and are very bulky. For example, the authors in [94], [102] utilized the MEDAV RUSK sounder for UAV channel measurements. This commercial channel sounder was placed on the ground and connected to the UAV via a 600-meter optical fiber. This solution has high reliability but is complicated and risky, thus it has not been widely adopted.

Another option for the UAV channel sounder includes the portable signal generator (as an aerial transmitter) [34] and the portable spectrum analyzer or network scanner (as an aerial receiver) such as Rohde Schwarz TSMA mobile network scanner [82], [85], Anritsu MS2760A-0100 spectrum analyzer [110], and SAF Tehnika J0SSAP14 spectrum analyzer [112]. In [34], the authors did not provide the specific model of the utilized signal generator. Thus, we surveyed portable signal generators in the market and found some potential ones such as Signal Hound VSG25A/60A and SHF 78124A. The portable signal generator is a suitable instrument as the aerial transmitter, which can generate some built-in waveforms as well as load customized sounding signals. In [34], a vector signal generator was mounted on a small-size aircraft and generated a 20 MHz chirp signal with a center frequency of 5060 MHz. The measured strengths and channel impulse responses (CIRs) were well extracted from the received signal. The spectrum analyzer (or network scanner) is convenient to obtain the CTF and also has good receiving sensitivity which is beneficial for long-range measurements. However, for most channel measurements with the signal generator and spectrum analyzer, only CW power or scalar frequency response can be obtained, thus we cannot get CIR due to lack of phase information. Moreover, these instruments have limited RF ports and are not suitable for multiple-channel measurements with an antenna array. Considering a dynamic UAV channel measurement, the frequency sweeping time (especially in a wideband channel sounder) should be shorter than the channel stationary interval. Although frequency sweeping with a few measurement points can be very fast, it will shorten the coverage range of the measured path delays. The maximum

path delay is determined by

$$\tau_{\max} = \frac{1}{\Delta f} = \frac{N_f}{B} \tag{1}$$

where $\Delta f$ is the frequency sweeping interval, $N_f$ is the number of measurement points, and $B$ is the bandwidth of the channel sounder.

*2) Off-the-shelf communication devices:*

For some communication systems, i.e., WLAN and cellular mobile communication, channel estimations are performed in the receiver with the help of predefined pilots. Therefore, the channel response can be obtained from the data packet directly. For example, an 802.11abgn module from SparkLAN WPEA-127N was used on a quadrocopter UAV in [69]. By communicating via IEEE 802.11a wireless LAN to the ground access point, the received signal strength was extracted from the test data packets, and then the channel characteristics of aerial links, i.e., path loss and small-scale fading were analyzed. In [113], a Xiaomi smartphone compatible with 5G bands was mounted on a quadcopter drone of DJI Matrice 210 to perform the cellular-to-UAV channel measurement. The received signal strength was easily recorded via a Tems Pocket application. These types of communication devices usually estimate the channel based on the pilot sequences in data packets. They have limited channel sounding capability because only limited bandwidth resource and symbols are allocated for pilot sequences. Note that two series of UWB radio devices, the DWM1000 series [97], [103], [114] and the Time Domain P410/440 series [74], [101], [109], [112] were widely used in UAV channel measurements. These UWB radios can measure CIRs with high delay resolution due to the GHz-level bandwidth.

In general, these off-the-shelf communication devices are easy to use without extra hardware implementation and signal processing. Moreover, thanks to the excellent manufacturing technology and high integration, they usually have small volumes, light weights, and low power consumption. In [99], a Facebook Terragragh radio device was utilized to perform A2A mmWave channel measurements. This device has a center frequency of 60 GHz and an array of $36 \times 8$ antenna elements, and it can be easily mounted on a DJI M6000 UAV. The flip side of high integration is that it is less flexible for users to upgrade hardware components or develop their own algorithms for specific measurement requirements.

*3) Portable SDR modules:*

In existing works, SDR modules are mostly used in UAV channel sounders for their high generality and flexibility. Different from the off-the-shelf communication devices, users need to design and implement the signal processing algorithms of channel sounding. According to our survey, this kind of system can be divided into two categories, i.e., commercial USRP and customized SDR modules. Most commercial USRPs used in UAV channel sounders are National Instruments (NI) USRPs (also called Ettus Research USRPs in some references), e.g., USRP B210 [76], [91], N210 [89], X310 [116], and 29XX series [105]. Besides, the commercial SDR modules of BladeRF 2.0 are also available solutions for UAV channel measurements [117]. These USRPs need to work with a laptop or an integrated central processing unit (CPU). There are also some redundant hardware components that are not designed for channel measurements. To further ease the burden of UAV payload and power consumption, some researchers developed simplified SDR modules based on FPGA development boards [92], [123], which are usually smaller, lighter, and cheaper. However, it involves extra hardware and software development and implementation, and the RF specifications might not be as good as commercial products.

### *D. Antenna configurations for "propagation channel" measurements*

The gain patterns of the transceiver's antennas significantly affect the path power of the measured channel. For simplicity, we define the wireless channel involving the antenna effects as a "radio channel" in this paper. Otherwise, it is a "propagation channel." From the perspective of channel modeling, we usually need the "propagation channel" model so that it can be combined with any antenna pattern. For example, the antenna patterns are modeled as an independent part in some UAV channel models [12], [141]. In this case, an essential goal of UAV channel measurement is to capture the characteristic of the "propagation channel". The challenge is that it is hardfor UAV channel sounders to retrieve propgation channel from the radio channel, i.e., antenna de-embeding. We need to know the multipath profile and the antenna pattern to perform the de-embeding process. However, it is not easy to capture the multipath profile with complete angular information for a sounding system with single antenna or few antenna elements on the drone. The antenna pattern should also be measured with consideration of the UAV airframe.

On the contrary, some UAV measurement campaigns aimed at capturing the "radio channel" for specialized applications [89]–[91], [93]. For example, the authors in [89], [90] utilized the commercial base stations (BSs) as transmitting part to capture the radio channels. As the antenna specifications of these commercial BSs were unknown, the effect of antenna properties was included in the measured results. Their results are valuable for understanding the downlink channels of cellular-connected UAV communications in the specific measurement region. The drawback is that when the antennas are upgraded afterward, the measured results might not be applicable anymore. Therefore, in this section, we focus on discussing the antenna configuration for capturing the "propagation channel".

*1) Antenna pattern affected by UAV airframe:*

Compared with terrestrial communications, UAV communications experience more variations in elevation angles due to variant flight height. In other words, the measured UAV channels are more sensitive to the change of elevation antenna pattern. For instance, the authors in [100] equipped the ground station with an omnidirectional antenna and a directional antenna with a 120° and 30° elevation pattern at half-power beam width (HPBW), respectively. They found that the directional antenna had a more significant impact on the measured channel characteristics, i.e., path loss and $K$-factor, and made the measurement results irregular. Therefore, most UAV channel

sounders at sub-6 GHz bands utilized omnidirectional antennas as shown in Table II. Note that these omnidirectional antennas have approximately perfect azimuth patterns, usually with less than 120° elevation patterns at HPBW. The propagation paths could still drop into the nulls of antenna pattern. Thus, a proper flight trajectory of the UAV needs to be designed to avoid this.

In addition, some propagation paths impinge the UAV airframe when using the omnidirectional antenna at the UAV side, so UAVs with different airframe shapes would affect the radiation patterns differently. Very recently, some research on UAV channel modeling began to consider the effect of UAV airframes to improve the accuracy of channel models [10]. It is necessary to remove the effect of UAV airframe on the radiation pattern. Some works take the antenna and UAV airframe as a whole to obtain the equivalent radiation pattern via field measurement in the anechoic chamber [83], [87] or simulation tools [48], [123]. For example, the authors in [87] found that the radiation patterns at the UAV side were less uniform due to the effect of airframe. Some deviations with null patterns for the antenna can be found in [48]. In our previous work [123], we simulated the equivalent radiation patterns for the antenna mounted at the bottom of UAV airframe and a rotary wing, respectively. As shown in Fig. 5, for this UAV airframe, we found that mounting the antenna at the bottom of UAV fuselage is a better choice, but the vertical plane of equivalent antenna pattern is still less uniform than the theoretical one. Since the deviation of antenna gain could reach more than 10 dB, it needs to be removed from the measurement results. Generally speaking, the effects of UAV airframe and antenna placement on the equivalent antenna pattern have rarely been discussed in the existing UAV channel measurement campaigns.

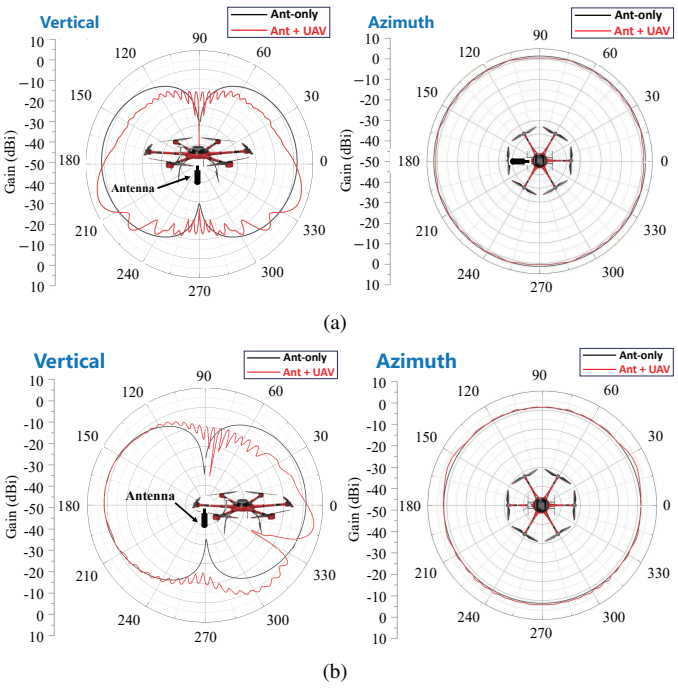


Fig. 5. Antenna pattern affected by the UAV airframe with an antenna on the bottom of (a) the fuselage and (b) a rotary wing.

*2) Directional antenna scanning:*

For high-frequency bands, especially the mmWave band, directional antennas are utilized to compensate for the high propagation power loss. At the same time, in the channel measurements, the directional antenna manages to capture channel spatial information at specific angles. For instance, the authors in [120], [121] equipped the UAV channel sounder with a directional antenna to measure the power of a target propagation path, so the interference of other multi-paths can be excluded. When aiming to measure the "propagation channel", the directional scanning sounding (DSS) method is widely used in terrestrial channel measurement campaigns [142]–[144]. This solution can also be found in UAV channel sounders [112], where a directional horn antenna was mounted on the UAV for mmWave channel measurement. This horn antenna can be rotated vertically via a dedicated servo control, while the UAV posture rotation can realize the azimuth rotation of the antenna. In this way, the power-angle profiles were obtained directly without performing angle estimation.

However, several issues must be considered when adopting the DSS method in UAV channel sounders. Firstly, UAV channel sounding has a particular issue: the vibration produced by the propellers (i.e., wobbling) when the drone is moving or hovering [145], [146]. This vibration may impact the coherence time of the wireless channel between UAVs and ground user equipment (UE). In [147]–[149], this effect is analyzed, and it was observed that even for slight UAV wobbling, the coherence time of the channel may degrade quickly, causing difficulties when tracking the channel to establish a reliable communication link. Fig. 6 shows an experimental example of this effect, where the power of the strongest peak was evaluated under two conditions while the drone was hovering and when the propellers were turned off [105]. The standard deviation of the LOS bin power for the hovering case is 0.48 dB compared to 0.08 dB when static, which confirms the conjecture that the hovering creates additional variations compared to the static case. This effect translates to any estimated parameter coming from the UAV campaign. Fig. 7 compares the RMS delay spread obtained from a drone with the propellers on (hovering) against the case when they are off (static). Like the previous case, the variation observed in the hovering case is larger compared to the static case one (2.74 times larger). The previous results demonstrate how important it is to consider the impact of wobbling and how it might affect further results obtained from a UAV campaign. In [146], [150], the wobbling was proved to obey Gaussian distribution via field measurements. Therefore, it is necessary to mitigate the effects of these fluctuations on the scanning accuracy, especially for long-distance UAV channel measurements.

Secondly, it is a big challenge to determine the scanning step and merge the channel data for the DSS method since the main lobe and side lobe of antenna pattern may overlap. The aforementioned UAV's fluctuations would make it even worse. Moreover, the stationary interval (SI) of UAV channels is typically second-level or even millisecond-level [151]. It takes a long time for the mechanical rotator to scan the whole 3D channel space. Therefore, faster scanning schemes like multi-antenna switching or 3D beam former are needed. More-

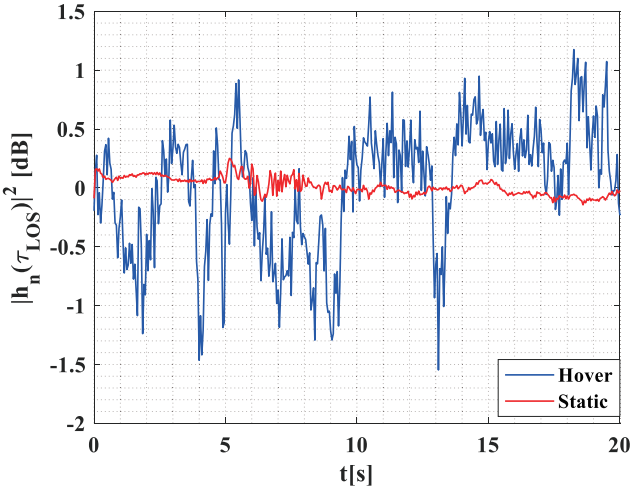


Fig. 6. Comparison of the normalized peak power in the PDP in LoS UAV scenario [105].

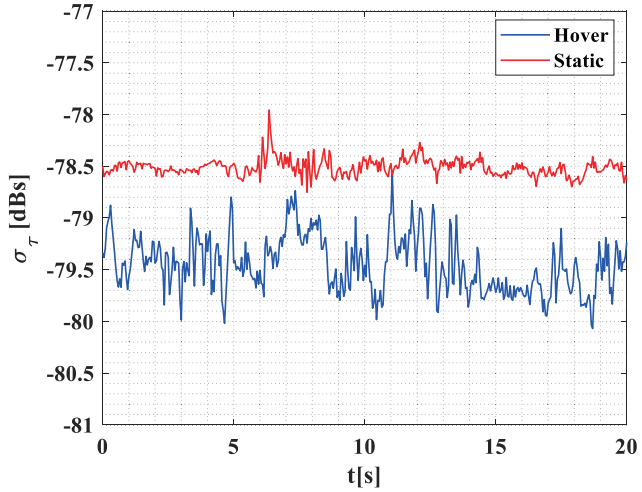


Fig. 7. Comparison of the RMS delay spread in LoS UAV scenario [105].

over, how to accurately suture several time-variant channel snapshots (captured from different angles) into one complete channel response needs to be tackled. According to existing works, the above issues have not been fully discussed and addressed under the scope of UAV channel measurements.

## III. Sounding Schemes of UAV Channel Sounders

According to the sounding signal types, the existing UAV channel sounding schemes can be divided into several categories, i.e., continuous wave (CW)-based, pulse-based, chirp-based, WLAN/cellular-based, and correlation-based channel sounding schemes. These sounding schemes are also typical in terrestrial channel sounders. However, the sounding signals need to be specially designed (i.e., bandwidth, length, snapshot duration, snapshot number, etc.) to achieve proper sounding capabilities for target UAV measurement scenarios such as delay resolution, maximum path delay, Doppler resolution, maximum Doppler frequency, etc.

### A. CW-based UAV channel sounder

CW is a typical sounding signal that has constant amplitude and frequency. It can be used to easily measure the received power (e.g., via a signal analyzer) and further analyze the large-scale channel fading (LSCF) characteristics, such as path loss (PL) and shadowing. CW has also been considered a proper sounding signal in the narrowband communication systems to capture the statistical distributions of small-scale channel fading (SSCF) [83]. For example, the authors in [98] utilized the CW signal to perform UAV-to-ground channel measurements at multiple frequency bands, i.e., 1 GHz, 4 GHz, 12 GHz, and 24 GHz. The received powers were recorded via a spectrum analyzer. By averaging the received power with a 20-wavelength sliding window, the LSCF characteristics such as PL and shadowing were analyzed and modeled. Then, the SSCFs were obtained by removing the LSCFs from received signals, from which the statistical properties, i.e., probability density function (PDF), cumulative distribution function (CDF), level crossing rate (LCR), and average fade duration (AFD) were calculated and analyzed. Therefore, the CW signal is a suitable sounding signal for measuring the power-related channel characteristics, where signal generation and data post-processing are both simple. However, as a single-tone power-only measurement, it cannot distinguish channel multi-path components (MPCs).

### B. Pulse-based UAV channel sounder

The narrow-pulse-based sounding scheme is an easy way to capture the channel MPCs directly without complex data processing. According to our survey, most existing pulse-based UAV channel sounders are based on the DWM1000 ultra-wideband (UWB) radio or Time Domain P410/P440 UWB radios [74], [101], [103], [109], [112], [114]. It can be found that all these measurement campaigns are carried out within a short range, e.g., within 100 m. The pulse signal has a short time duration and can be used to extract the CIR snapshot quickly, which is suitable for capturing time-variant CIRs of UAV channels. However, the pulse signal has a large peak-to-average power ratio (PAPR) and a low transmission efficiency. Therefore, the pulse signal needs high transmitting power for long-distance channel measurements, which would increase the burden of the UAV battery life..

### C. Chirp-based UAV channel sounder

The chirp signal is known as frequency modulated continuous waveform (FMCW), in which the frequency decreases or increases with time. The chirp signal can be applied for both time-domain and frequency-domain channel measurements. In the time-domain measurement, a linear chirp signal is generated at the transmitter. A mixer at the receiver is used to extract the frequency deviations between the received signal and the local chirp signal. These frequency deviations correspond to the propagation delays of each channel MPC as shown in Fig. 8. This time-domain solution has been widely used in the FMCW radar to measure the distance of target objects [152]. However, different from radar systems, the

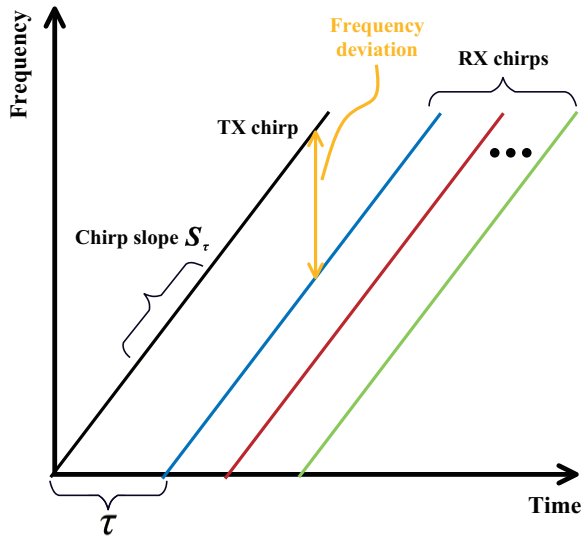


Fig. 8. Illustration of the chirp-based sounding scheme in the time-domain.

UAV channel sounder usually has distributed transceivers thus resulting in a poor phase alignment, which cannot meet the high requirements of phase accuracy in the chirp-based time-domain scheme.

In most of existing UAV channel sounders, chirp signal is utilized in frequency-domain channel measurements [29], [34], [117]. The frequency spectrum of the received signal is used to extract the channel transfer function (CTF), from which the CIR can be obtained by performing the inverse fast Fourier transform (IFFT). In [34], a chirp signal with a bandwidth of 20 MHz was designed and transmitted via a vector signal generator at the center frequency of 5060 MHz. The received signals were recorded in a signal analyzer, from which CIRs were calculated and analyzed. As these chirp-based frequency-domain schemes run in a swept-frequency way, they can sweep over a large frequency range without the limitation of instantaneous bandwidth. However, it will take some time to scan over a large bandwidth. For highly dynamic UAV communication scenarios, the scanning time should be shorter than the stationary interval of time-variant UAV channels. Although we can increase the scanning speed by reducing frequency points, it will decrease the measurement capability of maximum path delay.

### D. WLAN/cellular-connected UAV channel sounder

In the existing WLAN/cellular-based channel sounders, the mainly used sounding scheme is OFDM technology [77], [81], [105], except for some old communication standards like global system for mobile communications (GSM), high-speed packet access (HSPA), and universal mobile telecommunication system (UMTS) [63], [79]. The OFDM-based channel sounding scheme is a typical multi-tone sounding scheme. Independently modulated subcarriers in the OFDM system are employed for frequency-domain channel measurements. The CTF (also called channel state information) can be obtained directly from the OFDM data packet along with the actual communications. It has a good flatness of frequency spectrum but has a large PAPR. The authors in [81] developed an OFDM-based UAV channel sounder with subcarriers varying from 64 to 2048. An optimized QPSK sequence carried by the subcarriers was designed to reduce the PAPR. During the measurement, OFDM packets were continuously transmitted with an inter-packet interval. The CTF and CIR were then extracted from each received OFDM packet. Moreover, as OFDM technology has been widely used in cellular mobile communications, commercial BSs can be taken as one part of the channel sounder. For example, the developed channel sounder in [89] received the downlink signals from several commercial BSs in the measurement scenario. The CIRs were extracted from the cell-specific reference signals in each downlink frame.

Based on off-the-shelf WLAN/cellular communication devices, OFDM is an easy solution for channel measurements. In addition, these devices usually have a high level of integration and thus are small, lightweight, and low power, which is perfect for UAV platforms to carry. However, it consumes some uncontrollable time to deal with OFDM frames in these communication devices, which brings a challenge to measure a highly dynamic UAV channel with a small stationary interval.

### E. Correlation-based UAV channel sounder

In the correlation-based channel sounder, the sounding signal is carefully designed and its autocorrelation can be well approximated by a delta function. Thus, the CIR can be obtained by performing the sliding correlation operation at the receiver as

$$\begin{aligned}\hat{h}\left(t,\tau\right) &= y\left(t\right) \otimes s\left(t\right) \\ &= h\left(t,\tau\right) * s\left(t\right) \otimes s\left(t\right)\end{aligned} \tag{2}$$

where $s\left(t\right)$ is the sounding signal, $y\left(t\right)$ is the received signal, $h\left(t,\tau\right)$ is the real channel under measurement, $*$ is the convolution operator, and $\otimes$ is the sliding correlation operator.

The commonly used signals include ZC sequence and PN sequence. As a digital binary sequence, the PN sequence needs a shaping filter to make it suitable for subsequent modulation and transmission. However, the ZC sequence is suitable to be modulated and transmitted directly. In addition, different primitive polynomials are needed for generating PN sequences with different types and lengths to balance the data length and dynamic range of the measured CIR snapshot. For example, when generating an m-sequence with a length of 10, we use the primitive polynomial "$x^{10}+x^3+1$". The ZC sequence has a uniform generation function as [153]

$$s[n] = \begin{cases} \exp\left(-\frac{\mathrm{j}\pi\mu n^2}{N_{\mathrm{ZC}}}\right) & N_{\mathrm{ZC}} \text{ is even number} \\ \exp\left(-\frac{\mathrm{j}\pi\mu n(n+1)}{N_{\mathrm{ZC}}}\right) & N_{\mathrm{ZC}} \text{ is odd number} \end{cases} \tag{3}$$

where $n = 0, 1, ..., N_{\mathrm{ZC}}-1$, and $N_{\mathrm{ZC}}$ is the sequence length. Note that $\mu$ is less than $N_{\mathrm{ZC}}$ and relatively prime to $N_{\mathrm{ZC}}$.

In [123], [154], it was stated that the ZC sequence has better spectrum flatness. Moreover, it was pointed out in [155] that the ZC sequence has a better autocorrelation property than the PN sequence, while the opposite conclusion was

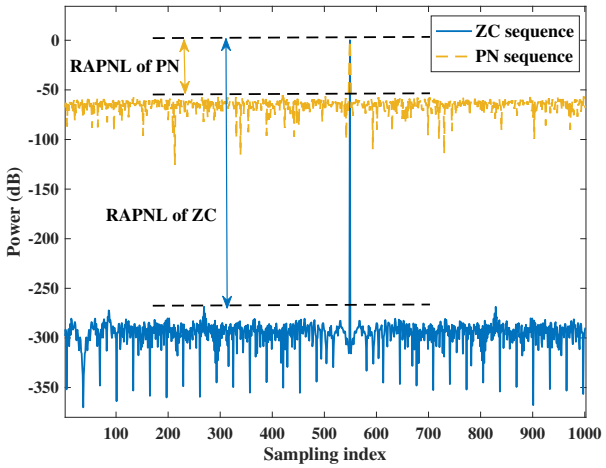


(a)

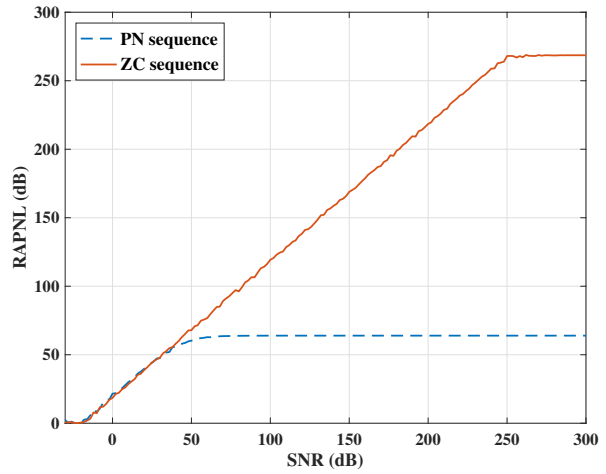


(b)

Fig. 9. Comparison of RAPNLs for ZC and PN sequence (a) without noise and (b) under different SNR conditions.

drawn in [154]. To clarify this, we performed a comparison test regarding the ratio of autocorrelation peak to noise level (RAPNL) without noise and under different signal-to-noise ratio (SNR) conditions, as shown in Fig. 9. The length of both the PN and ZC sequences is set as 1024 and the bandwidth of generated sounding signals is 100 MHz. It was found that the ZC sequence has a better theoretical performance of autocorrelation property than the PN sequence. However, they share a similar performance of autocorrelation property under typical SNR conditions, e.g., below 30 dB.

For the sliding-correlation-based sounding scheme, the dynamic range of measured CIR can be increased by adopting a longer sounding sequence, which can capture more UAV channel MPCs. However, the measurement time of each CIR snapshot would increase in this case. Therefore, a balance between dynamic range and measurement time needs to be achieved accordingly when applying this scheme to the UAV channel sounder.

### *F. Summary and Comparison of different channel sounding schemes*

In Fig. 10, we summarize the sounding signals utilized in the existing UAV channel sounders [21]–[123]. Note that some references did not present sounding signals used in their channel sounders, so they are not listed in Fig. 10. It can be found that the OFDM signal is the most popular one as it has been widely used in cellular mobile communications and WLAN communications, and the chirp signal is the least one. The correlation-based sounding scheme also shows great potential. To present the pros and cons of each sounding scheme, we analyzed the performance of different sounding signals regarding signal generation, data post-processing, speed (how fast each measured channel snapshot can be updated), and so on in Table IV. Compared with the chirp-based and correlation-based sounding schemes, the OFDM-based sounding scheme is faster to obtain a CIR snapshot. It is because the frequency responses of pilot subcarriers in the OFDM frame are captured parallelly while the other two schemes need at least a whole duration of the chirp signal or the ZC/PN sequence. But, when the OFDM-based channel sounding is performed along with the communication, the sounding speed will slow down because the cycle prefix is needed ahead of each OFDM symbol and it will consume some time to deal with the header of each OFDM frame. The correlation-based sounding scheme achieves a good balance of complexity, speed, and transmission efficiency. The CW signal is perfect if you focus on power-only measurements.

## IV. Synchronization, Calibration, and Optimization of UAV Channel Sounders

### *A. Transceiver synchronization*

The transceivers of the UAV channel sounder separate far away from each other, so it is hard to provide a common clock over a long range. In [94], [102], the authors placed the radio frequency (RF) transceivers together on the ground and synchronized them with a common rubidium clock. However, the UAV was connected via a 600-meter optical fiber for long-range measurements. This fiber-based solution enables perfect transceiver synchronization, but extra electrical-to-optical and optical-to-electrical devices are needed. Moreover, it is a challenge to guarantee flight security when mounting a fiber on a moving UAV. Therefore, this section discusses the commonly used solutions for time and frequency synchronization in the existing UAV channel sounders with separate transceivers.

*1) Time synchronization:*

In the channel measurement, it is desirable to synchronize the initial starting point of the transmitted sounding signal with the receiver's sampling (i.e., time synchronization), thus allowing the measurement of the absolute delay of MPCs [46]. It is also beneficial for aligning the channel measurement data with designed events like global positioning system (GPS) positions or UAV postures. The existing solutions include the global positioning system (GPS)-based [65], [66], [92], disciplined-oscillator-based [26], [88], [100], and data-packet-based synchronization schemes [30], [89], [101].

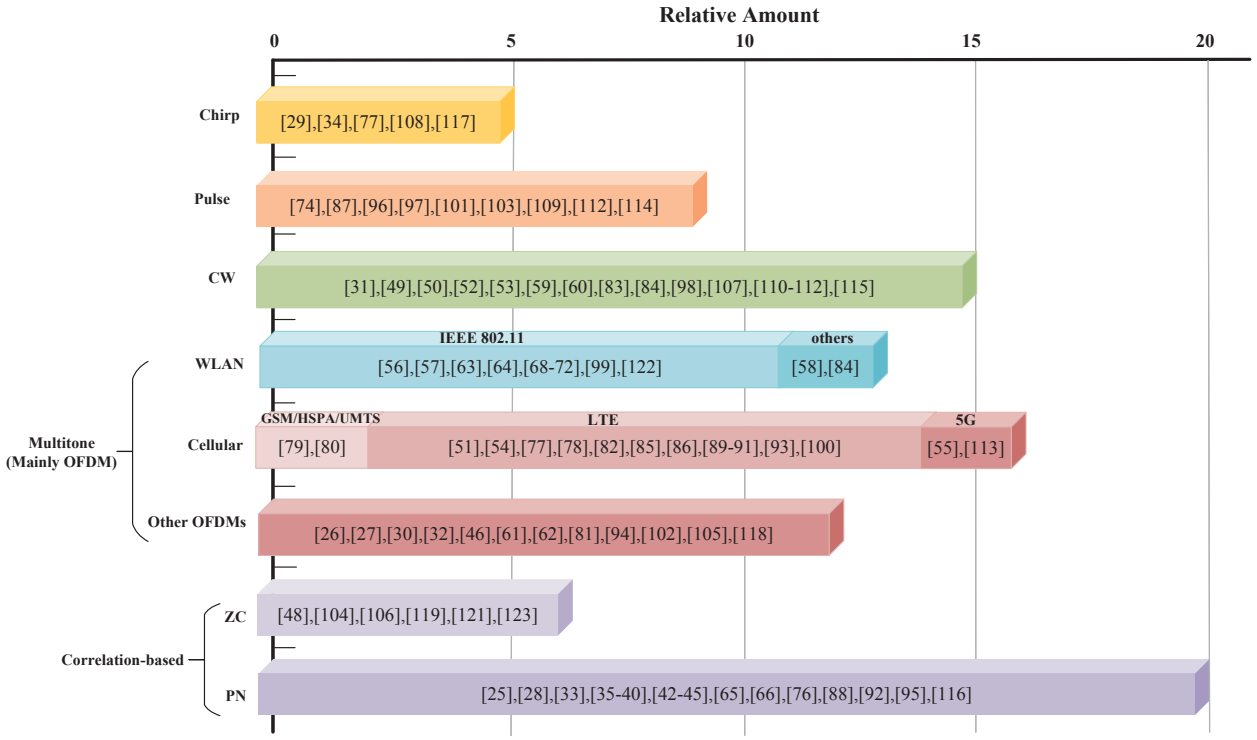


Fig. 10. Statistics of sounding signals utilized in the existing UAV channel sounders.

TABLE IV
PERFORMANCE COMPARISON OF DIFFERENT SOUNDING SIGNALS.

| Sounding Signal | | Signal Generation | Data Post-processing | Speed | PAPR | Others |
|---|---|---|---|---|---|---|
| CW | | ★★★★★ | ★★★★★ | ★★★★★ | ★★★★★ | Single-tone power-only meas. |
| Pulse | | ★★★ | ★★★★★ | ★★★★ | ★ | Short transmission distance |
| Chirp | | ★★ | ★★★★ | ★(sweeping)<br>★★★ (time domain) | ★★★★ | Sweep over a large frequency range |
| WLAN/Cellular (OFDM) | | ★ | ★★★ | ★★★★ | ★★ | Many commercial options |
| Correlation | ZC | ★★★★ | ★★ | ★★★ | ★★★★ | • ZC has better spectrum flatness<br>• Similar autocorrelation property |
| | PN | ★★★ | ★★ | ★★★ | ★★★ | |
| Note: more ★ means better performance. | | | | | | |

For the GPS-based scheme, the transceiver is triggered by the GPS time or one pulse per second (1PPS) signal. The GPS module is low-cost and easy to use, and the GPS module in the UAV navigation system can be shared with time synchronization. The 1PPS signal could bring a nanosecond-level deviation for the time synchronization, but it is acceptable for most channel sounders. However, this scheme cannot be used in some GPS-denied environments.

In the disciplined oscillator scheme, high-precision oscillators such as rubidium oscillators at the transceiver are disciplined by a reference source like a GPS signal. It has a precision of picosecond but is more expensive and usually takes several hours to discipline the rubidium oscillators. In addition, the accuracy of disciplined oscillators would decay gradually after disconnecting from the reference source due to the limited holdover time.

The data-packet-based scheme is a type of software synchronization scheme. One way is to transmit the data packet that contains the clock information or specific synchronization signals, such as the primary and second synchronization signals in OFDM-based channel sounders [89]. Another way is to transfer a data packet in a bidirectional communication mode to estimate the time of flight (ToF), which can be eliminated in the data post-processing [157]. This solution does not need extra hardware components and thus is more flexible. However, the time consumption that the software processes the data packet is not controllable, which could bring some deviations in the time synchronization. In the bidirectional communication mode, the UAV motion will also make it hard to estimate the ToF accurately.

*2) Frequency synchronization:*

In the separated transceivers, there is a frequency offset (also called clock drift) between two local oscillators due to imperfect manufacture. Taking a 40 MHz crystal oscillator as

an example, if the frequency deviation is 15 parts per million (PPM), the maximum frequency offset between transceivers can reach up to 1200 Hz. In [47], [123], it has been proved that the sampling frequency offset (SFO) would cause a periodic power loss of the measured MPCs in the correlation-based channel sounders. A delay shifting of measured power delay profile (PDP) caused by the SFO was also observed in [95]. Most of common solutions are similar to those utilized in time synchronization. High-precision reference clocks provided by the GPS module or disciplined rubidium oscillator are used to minimize the frequency offset [34], [88], [95]. However, as stated in [123], the power loss caused by the SFO is cumulative, so the issue still exists over a long-time measurement despite of small SFO. In [95], although the GPS-disciplined oscillator was used, the delay and Doppler shift were still observed. Another solution is to compensate for the effect caused by the SFO in the data post-processing. More discussions about SFO compensation methods in the data post-processing can be found in Sec. IV.C.

Note that some OFDM-based channel sounders also have the capability of carrier frequency synchronization, which is used to correct the carrier frequency shift. It is beneficial for OFDM communications, but it may ruin the channel Doppler information since the carrier frequency shift could be partly caused by the Doppler effect. Therefore, this factor must be carefully considered when developing an OFDM-based UAV channel sounder.

### B. Calibration and verification

To ensure the reliability of channel sounders, preliminary calibrations and verifications are required before conducting field measurement campaigns. The commonly used calibration and verification methods for UAV channel sounders are summarized as follows.

*1) Preliminary calibration:*

• **Power calibration.** PL is an important parameter for channel measurements, which is defined as the power difference between the transmitted and received signals. Therefore, the channel sounder should accurately detect the power difference. In [72], the measurement devices were placed in a Rodhe & Schwarz shielding box. They were interconnected with a rotary step attenuator, and the attenuation increased by 1 dB every minute. In [99], the channel sounder was placed in a temperature chamber. Under different temperature conditions, it was calibrated through a calibrated NI transceiver system, which could accurately report the absolute incident power and isotropic radiated power. If power errors are detected in these calibration tests, they would be compensated in the subsequent data processing or by calibrating the hardware components.

• **Phase calibration.** For a multiple-input multiple-output (MIMO) channel sounder, the angular information is estimated according to the relative phase differences of received signals from different radio frequency (RF) chains. Therefore, it is crucial to initially align the phases of all channel sounder's RF chains. In [123], a signal generator that outputted a sine waveform was connected to all the RF chains via a power splitter. The phases of received sine waveform in each RF chain were compensated to the same value. After calibration, the phase deviations of different RF chains were below 0.2° at the 3.5 GHz frequency band. This method is easy to perform but it does not consider the effect of antenna properties on the phase calibration. A wireless calibration method was utilized in [54]. An antenna element in the center of the antenna array was used to transmit a sine wave. Taking the received phase of one antenna element as a reference, the phases of other antenna elements were compensated. The phase deviations were less than 1° at the 1.8 GHz frequency band. This solution takes the antennas into account, which is more consistent with the realistic measurement environment. However, the calibration results via the over-the-air method are probably affected by surrounding environments.

• **Back-to-back (B2B) calibration.** In the channel measurement, we only need the response of the propagation channel and antennas [105]. However, the response of hardware components, i.e., filters and amplifiers, are always included in the measured data. Therefore, back-to-back (B2B) calibration is necessary before the field measurement [65], [92], [105], [123]. In the B2B calibration, the transceivers of the channel sounder are connected directly via an RF cable. The hardware system response can be obtained by performing a channel measurement procedure, and then it can be eliminated from the measured CIRs by data post-processing in the field measurement. The details can be found in Sec. IV.C.

*2) Preliminary verification:*

The calibration procedure mainly aims at the hardware components or one specific channel parameter. After the calibration, a comprehensive test is needed to verify the reliability of the final output of the channel sounder, which involves both the hardware and the software algorithm. The existing verification methods for UAV channel sounders are summarized as follows.

• **Qualitative verification.** In this verification method, a preliminary channel measurement campaign is performed under scenarios that have some widely accepted theoretical results such as reliable RT simulations. In [87], RT simulation results were used for verification. In the RT simulation, the shapes and positions of scatterers in the measurement scenario were accurately reconstructed, and the material coefficients such as the permittivity and conductivity were preset by the authors. The RT simulation results, i.e., PLs, shadowing, RMS delay spread, and multi-path number were compared to the measured ones, which proved the reliability of the developed UAV channel sounder. Note that in these verifications, the measured results are statistically compared with the theoretical ones. Therefore, it is typically a qualitative verification method.

• **Quantitative verification.** This method utilizes other commercial instruments to validate, such as vector network analyzers (VNAs) and channel emulators. The VNA has been well-known for channel measurements, so the measured results by VNA can be used to verify other channel sounders in the same environment. For example, a verification test was performed in a conference room at 2.3 GHz and 5.8 GHz [81]. The same channel impulse response was captured by the UAV channel sounder and VNA-based sounder, respectively.

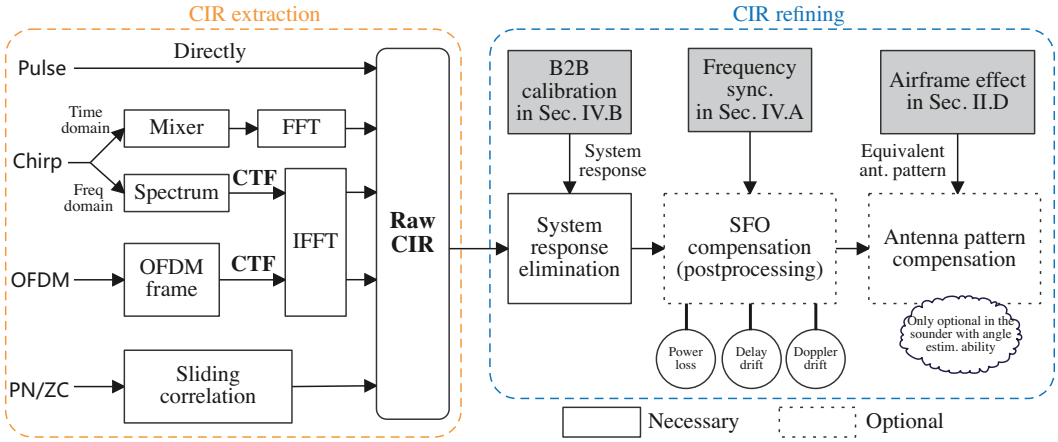


Fig. 11. A typical framework for CIR extraction and refining.

The measured amplitudes of MPCs by two systems were close to each other, which verified the effectiveness of the developed channel sounder. On the other hand, channel emulators can reproduce accurate and repeatable channels, which is a valuable tool to quantitively verify the performance of channel sounder [104], [123], [157]. In [157], the transceivers of the developed channel sounder were connected to a channel emulator. The channel emulator generated a three-tap channel with different tap power gain, delay, fading type, and Doppler spectrum. The power gain and delay of the measured PDP, the shape of the measured Doppler spectrum, and the measured fading distribution were compared with the preset values. Compared to the above qualitative verification methods, this verification solution is more of a quantitative method.

### C. Optimization for CIR measurements

According to our survey, the objectives of channel measurement can be divided into two categories: power-only measurements (e.g., received power, received signal strength (RSS), and RSS indicator (RSSI)) and CIR measurements (e.g., CTF and CIR). The power-only measurement can characterize power-related channel properties such as PL, shadowing, and fading distribution. Besides these, the CIR measurement can obtain MPCs that can characterize more channel properties like PDP, delay spread, K-factor, etc. For the power-only channel measurement, the power values can be easily recorded by the instruments or calculated by the received signals, while the data post-processing of CIR measurement is more complicated. Therefore, this section focuses on the extraction of CIRs and MPCs in the UAV channel measurements.

*1) CIR extraction and refining:*

The CIR extraction method varies with different sounding schemes introduced in Sec. III, as shown in the left segment of Fig. 11. However, the CIRs originally extracted from the raw channel data have some impairments due to imperfect hardware implementation. In the right segment of Fig. 11, we summarize some solutions utilized in the existing UAV channel measurements to refine the raw CIRs and obtain the accurate "propagation channel".

- **System response elimination.** In Sec. IV.B, we have discussed the B2B calibration method for obtaining the hardware system response. As it is complicated to perform the convolution operation in the time domain, most of research works eliminate the system response in the frequency domain [105], [116], [123]. It can be expressed as

$$h(t) = \mathrm{IFFT}\left(\frac{H(f)}{G(f)}\right) \tag{4}$$

where $H(f)$ and $G(f)$ are the frequency-domain response of raw CIR and the hardware system, respectively. In Fig. 12, we present a measured CIR affected by the system response in a developed channel sounder. The CIR is generated by a commercial channel emulator and measured by the developed channel sounder. It can be found that the noise level of the measured channel is increased, and some ghost MPCs occur. After the B2B calibration, the system response is well eliminated as shown in Fig. 12. Besides the elimination method, another way is to consider the system response in the signal model when conducting some high-resolution parameter estimation methods.

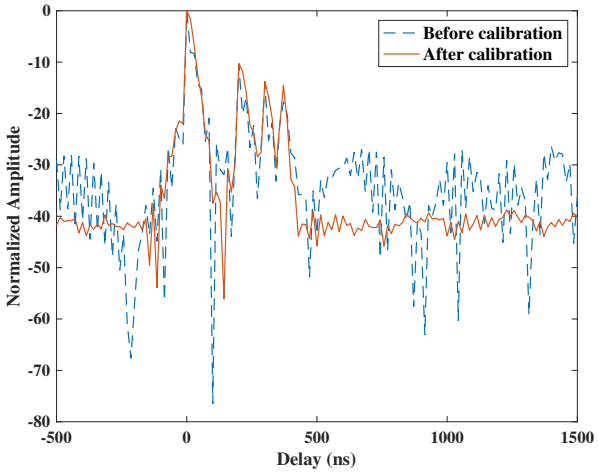


Fig. 12. B2B calibration of the measured CIR.

- **SFO compensation (post-processing).** In Sec. IV.A, fre-

quency synchronization methods for solving the SFO problem have been summarized. Some research works compensate the SFO from the hardware aspect, such as utilizing the high-precision oscillator clock, so the SFO compensation in the data post-processing is an optional solution. One existing solution tries to compensate for the SFO directly. For example, two fine sync symbols were integrated into the OFDM frame in [30]. The exported frequency estimation from the physical layer was used to perform an initial correction, and the residual frequency offset was then removed via an autocorrelation method. The authors in [157] proposed a frame exchange method where the sync frame contained clock timestamps. A synchronization algorithm was used to compensate the oscillator drift. Another solution aims to analyze the effect that the SFO brings to the measured results and then correct the results directly. For example, the effect of SFO on the amplitude of measured MPCs was compensated via a signal recovery method in [123], [156]. A post-processing method was proposed to correct the measured delay and Doppler shifting in [95]. This kind of solution avoids compensating the SFO itself, but the effects of SFO on different measured channel parameters in different sounding schemes need to be studied separately.

• **Antenna pattern compensation.** The UAV airframe may distort a quasi-isotropic antenna pattern and affect the path power of measured CIR. To obtain the CIR of propagation channel, the effect of the antenna pattern needs to be removed. Since the antenna pattern varies over different azimuth and elevation angles, the antenna pattern compensation is only optional for the channel sounders that are able to capture the angular information. In [110], antenna measurements were performed in an anechoic chamber, where the antenna was mounted on the UAV. The measured antenna patterns were interpolated over a mesh grid of azimuth and elevation angles and applied in the subsequent data post-processing. Under this condition, an enhanced effective aperture distribution method was found in [158] to recover patterns at arbitary angles. In [123], the antenna pattern affected by the UAV airframe was simulated via electromagnetic analysis software. The power of line-of-sight (LoS) path was compensated according to the antenna pattern and angular information. For the channel sounders without angle-estimation ability, the antenna position on the UAV needs to be carefully chosen to minimize the effect of UAV airframe. In [98], a proper flight trajectory was carefully designed to make sure that the angles of propagation paths were within a specific range. In this range, the antenna pattern did not change significantly.

*2) Noise thresholding for MPC extraction:*

The captured CIR snapshot from a measurement can be affected by noise from several sources. Each delay bin of the CIR may contain MPC information and noise. Noise, if untreated, may impact the estimation of parameters because noise can be treated as valid channel information (i.e., MPC).

We can use "Noise Thresholding" on the CIRs to minimize the errors produced by the noise. This method chooses a threshold, and the measured CIR samples below it are set to zero. The value can be selected with respect to the noise floor or the peak of the CIR. Several studies have been conducted in which a threshold to "cut off" the noise is implemented; the values selected range from 3 to 25 dB with respect to the average noise power or the CIR peak (see Table V). The threshold choice is critical because it may cause distortion in the estimated channel parameters (e.g., path loss, delay spread [159]). A high value may "cut off" desired MPCs to evaluate while leaving the threshold too low may allow noise to be treated as MPCs. A framework to evaluate the effect of noise in Fourier analysis is estimated, and the use of noise thresholding as a countermeasure is considered [160].

Most channel studies use a constant threshold strategy because of its simplicity in implementation [116]. However, in a UAV campaign, the SNR and peak power may differ while the drone is moving, affecting the detection of desired MPCs. A proposed alternative is the constant false alarm rate (CFAR) method, widely used in the radar, where dynamic thresholds are implemented on each delay bin, maintaining a constant false alarm probability [47], [123]. In Fig. 13, a comparison between the different noise thresholding methods is shown. A commercial channel emulator is used to generate the CIR snapshot with four valid MPCs, and then a channel sounder is applied to measure this predefined channel. It can be found that the constant noise thresholds are highly probable to miss some useful MPCs or bring in some fake MPCs. The situation will be worse for the time-variant CIRs. Note that all the above methods can only extract MPCs above the noise floor; future work in this area should discover strategies to remove MPCs below the noise floor in some low SNR conditions.

TABLE V
NOISE THRESHOLDING UTILIZED IN UAV CHANNEL MEASUREMENTS.

| References | Noise threshold |
|---|---|
| [34] | 10 dB higher than the median value of the CIR |
| [40] | 25 dB, 30 dB, 35 dB, and 40 dB lower than the peak power for comparison |
| [65] | 50 dB lower than the peak power |
| [47] | 25 dB lower than the peak power<br>False alarm probability of 0.01(CFAR) |
| [101] | 20% of the peak amplitude |
| [89] | 3 dB higher than the mean power of the noise level |
| [96] | 5 dB higher than the mean power of the noise level |
| [46] | 28 dB higher than the free space path loss |
| [123] | Dynamic noise threshold (CFAR) |

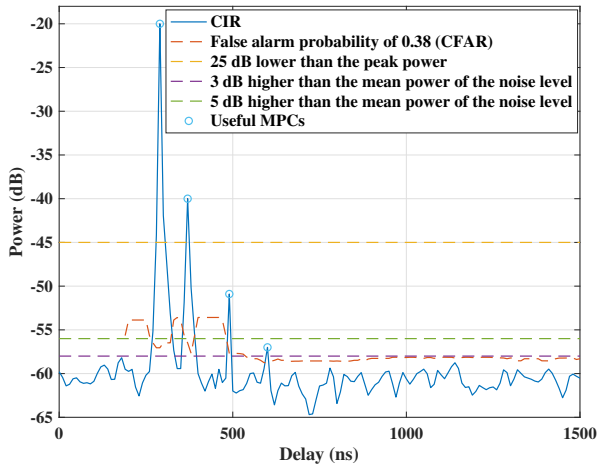


Fig. 13. Comparisons of different noise thresholds.

## V. Future Challenges and Open Issues

### A. UAV channel sounding for high-frequency bands

In future communication networks, it is claimed that the communication system will cover all frequency bands [161], [162]. For the high-frequency bands such as the mmWave band and sub-Terahertz (sub-THz) band, communication links are known to be tortured by the large power attenuation, especially in the NLoS scenarios [163]. Due to the flight flexibility of UAV in the 3D space, it is easier to have a LoS link for UAV-assisted communications than terrestrial mobile communications. Therefore, UAV-assisted communications at the high-frequency bands are promising in the future to support high data transmission rate. However, as discussed in Sec. II.B, UAV channel measurements have not been extensively performed at the mmWave frequency band, not to mention the sub-THz frequency band. Therefore, it is valuable to study UAV channel measurements at high-frequency bands. Several challenges and issues in developing a high-frequency UAV channel sounder are summarized as below.

• **Hardware implementation.** The high-frequency bands have rich bandwidth resources. In other words, communication systems at high-frequency bands normally have larger bandwidths. Currently, hardware components with high frequency and large bandwidth are expensive, complicated, and heavy. Some UAV channel sounders utilized portable mmWave spectrum analyzers [111], [112] and a portable mmWave test transmitter [98]. However, they can only be used to perform power-only channel measurements. In [99], the Facebook Terragraph radios were used to develop a UAV mmWave channel sounder. It worked at the center frequency of 60.48 GHz with a bandwidth of 2.16 GHz. It is not accessible to most researchers but is a good example for designing a highly integrated mmWave channel sounder.

• **Sounding scheme design.** A large bandwidth also brings a challenge to the sounding scheme. One method is to perform frequency sweeping during channel measurements (e.g., a chirp-based sounding scheme or a signal generator in the frequency-sweeping mode). This scheme can sweep over large bandwidth but consumes a lot of time, which is only suitable for stationary and quasi-stationary UAV channel measurements. The second scheme is sending a sounding signal with large instantaneous bandwidth (e.g., pulse-based, OFDM-based, and correlation-based sounding schemes). However, it is still a big challenge to deal with the baseband signal with such a high sampling rate so far.

• **Airframe shadowing.** The high-frequency signal has a short waveform length. Therefore, the UAV airframe would have a more severe impact on the signal propagation at the mmWave or sub-THz bands than that at sub-6 GHz bands. For A2G channel measurements, this impact can be minimized by carefully choosing the position of antennas on the UAV. For A2A channel measurements, the blockages by the UAV airframe are inevitable. Characterizing the shadowing caused by the UAV airframe especially rotating wings is worth studying for the high-frequency UAV channel measurements.

### B. UAV channel sounding for full-application scenarios

In the B5G and 6G communications, UAV platforms are expected to be combined with some other advanced technologies such as beamforming and reconfigurable intelligent surface (RIS) [164], [165]. It is also called "full-application scenarios" [166], [167]. Channel measurements for the beamforming-enabled and RIS-assisted UAV communications can help better understand the new features of propagation channels and assist the design and optimization of these communication systems.

The antenna array is normally utilized in mmWave or THz communications due to the high power attenuation. The beamforming technologies play an important role in these systems. According to the literature review, only the UAV mmWave channel sounder in [99] supported the beamforming technology. Both the transmitter and receiver were equipped with an antenna array with 36 $\times$ 8 antenna elements. The antenna array has a 90° coverage in the azimuth plane with 64 beam directions. Channel measurements were performed by scanning 400 beam pairs between two hovering UAVs. In this work, the UAV wobbling caused by the propeller rotation and wind was not considered. It may affect the beam steering direction and would become worse in a long-distance UAV channel measurement. Moreover, beam tracking is performed along with the UAV flight in the realistic beamforming communication systems, so this behavior should also be considered in the channel measurement campaigns in the future. As the UAV is moving, real-time beam-tracking is also a challenge when designing a UAV channel sounder.

RIS is a passive device to perform reflecting functionality to provide an efficient and robust communication link even in the NLoS scenario. In the RIS, each meta-surface can control the amplitude and phase of incoming signals, which would change the properties of propagation channel. The bright future of RIS-assisted UAV communications also boosts the studies on the corresponding propagation channels [168], [169], which need to be evaluated by the field channel measurements. To the best knowledge of the authors, no UAV channel measurement campaign involving RIS has been reported so far, which is a big research gap. In one potential measurement scenario, the

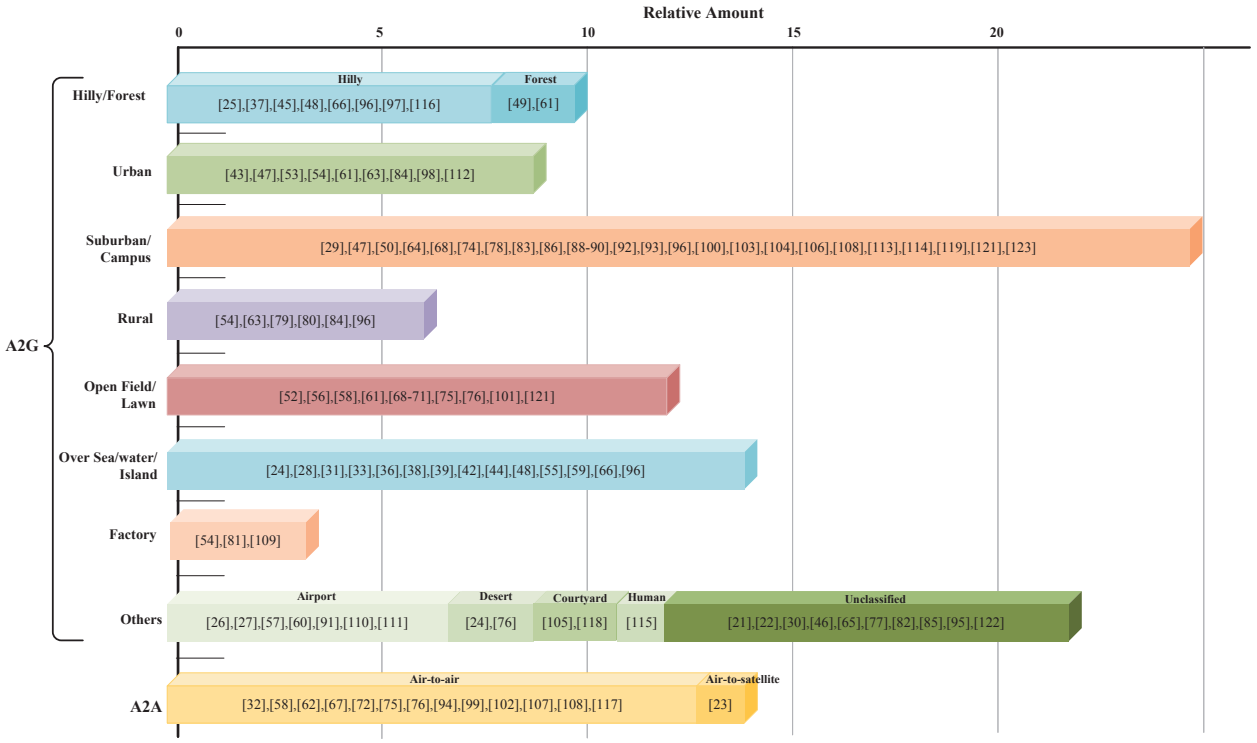


Fig. 14. Statistics of measurement scenarios.

RIS is placed on a fixed wall. The measured UAV channel is the superposition of the physical propagation channel and extra RIS-made channel. In this case, since the natural signal propagation process such as reflection and scattering behaviors are manipulated by the RIS, the signal model for some channel estimation methods becomes more complicated.

### C. UAV channel sounding for global-coverage scenarios

Future communication networks will cover all the scenarios, namely "global-coverage scenarios" [170]. As shown in Fig. 14, most existing UAV channel measurement campaigns are performed for the A2G or A2A links under some typical scenarios, i.e., urban, suburban, hilly, etc. However, more potential application scenarios of UAVs have been revealed recently, such as the smart factory scenario (also called industry 4.0) [171] and the 6G space-air-ground-sea integrated network (SAGSIN) [6]. These new application scenarios can be considered in further UAV channel measurements.

For the smart factory scenario, UAVs are considered valuable platforms to assist industrial tasks [171], where a reliable communication link is fundamental. According to our literature survey, only the work in [81], [109] involved the UAV channel measurements in a typical factory scenario. One of the reasons that UAV channel measurements are little in factory or industrial environments, is because of the need to not only communicate but also sense the obstacles with the help of other sensor modules like Lidar or camera. Although some factory scenarios can be viewed as a special case of indoor scenarios, the channel properties could be different due to the unique structures of factory buildings and machines. Therefore, UAV channel measurements under smart factory scenarios are needed. However, some GPS-based solutions for UAV channel sounders might not work anymore in these GPS-denied environments.

For the 6G SAGSIN, UAV is a bridge to link the other communication platforms, i.e., satellites, aerial nodes (e.g., airships and balloons), terrestrial nodes (e.g., BSs, cars, pedestrians, etc.), and over-sea nodes (e.g., ships) [6]. As the SAGSIN is still in the research phase, it is not feasible to perform a comprehensive UAV channel measurement involving all the communication nodes at present. The main challenge is that the UAV channel sounder needs to cover different frequency bands and support different communication schemes. Moreover, the interferences between the communication links of network also bring challenges to the data post-processing of UAV channel measurements.

## VI. Conclusions

In this paper, we have provided a comprehensive survey focusing on the UAV channel sounding technologies. From the hardware design of the channel sounder for UAV communications, we have summarized the key requirements for aerial platforms with highlighting the 6D motion and accessibility. Then, we have found that most research works focused on L-band and C-band for UAV channels, which leave much more space for future measurements at mmWave and sub-THz bands. In addition, antenna configurations for propagation measurements have been deeply discussed. At the software level, the sounding signals and data post-processing have been involved, which shows that OFDM-based sounding signal is the most popular one in the existing UAV channel sounders while correlation-based sounding signal has great potential.

We have also summarized possible solutions for synchronization and calibration since they are vital for obtaining accurate CIR. Finally, the challenges we are facing and opportunities for future UAV channel measurements have been highlighted, in terms of new frequency bands, new application scenarios, and new enabling technologies. The survey paper could facilitate a quick development of a UAV channel sounder, inspire more channel measurement campaigns, and provide new insight into UAV channels and communications.

## REFERENCES


[1] G. N. Muchiri, and S. Kimathi, "A Review of Applications and Potential Applications of UAV," in *Proc. SRIC'22*, Apr. 2022, pp. 280–283.

[2] A. M. Samad, N. Kamarulzaman, M. A. Hamdani, T. A. Mastor, and K. A. Hashim, "The Potential of Unmanned Aerial Vehicle (UAV) for Civilian and Mapping Application," in *Proc. ICSET'13*, Shah Alam, Malaysia, 2013, pp. 313–318.

[3] Allied Market Research, "Unmanned Aerial Vehicle (UAV) Market", Rep. A09059, Oct. 2021. [Online]. Available: https://www.alliedmarketresearch.com/unmanned-aerial-vehicle-market-A09059.

[4] P. Yang, X. Cao, T. Q. S. Quek, and D. O. Wu, "Networking of Internet of UAVs: Challenges and Intelligent Approaches," *IEEE Wirel. Commun.*, early access, pp. 1–11, Dec. 2022.

[5] C. Diaz-Vilor, A. Lozano, and H. Jafarkhani, "Cell-Free UAV Networks: Asymptotic Analysis and Deployment Optimization," *IEEE Trans. Wirel. Commun.*, early access, pp. 1–16, Oct. 2022.

[6] J. Liu, Y. Shi, Z. M. Fadlullah, and N. Kato, "Space-Air-Ground Integrated Network: A Survey," *IEEE Commun. Surv. & Tutor.*, vol. 20, no. 4, pp. 2714–2741, Fourthquarter 2018.

[7] B. Li, Z. Fei, and Y. Zhang, "UAV Communications for 5G and Beyond: Recent Advances and Future Trends,"*IEEE Internet Things J.*, vol. 6, no. 2, pp. 2241–2263, Apr. 2019.

[8] Q. Zhu, K. Mao, M. Song, X. Chen, B. Hua, et al., "Map-Based Channel Modeling and Generation for U2V mmWave Communication," *IEEE Trans. Veh. Technol.*, vol. 71, no. 8, pp. 8004–8015, Aug. 2022.

[9] K. Mao, Q. Zhu, M. Song, H. Li, B. Ning, et al., "Machine Learning-Based 3D Channel Modeling for U2V mmWave Communications," *IEEE Internet Things J.*, vol. 9, no. 18, pp. 17592–17607, Sept. 2022.

[10] B. Hua, H. Ni, Q. Zhu, C.-X. Wang, T. Zhou, et al., "Channel Modeling for UAV-to-Ground Communications with Posture Variation and Fuselage Scattering Effect," *IEEE Trans. Commun.*, vol. 71, no. 5, pp. 3103–3116, May 2023.

[11] Y. Liu, C. -X. Wang, H. Chang, Y. He, and J. Bian, "A Novel Non-Stationary 6G UAV Channel Model for Maritime Communications," *IEEE J. Sel. Areas Commun.*, vol. 39, no. 10, pp. 2992–3005, Oct. 2021.

[12] H. Chang, C.-X. Wang, Y. Liu, J. Huang, J. Sun, et al., "A Novel Non-Stationary 6G UAV-to-Ground Wireless Channel Model with 3D Arbitrary Trajectory Changes," *IEEE Internet Things J.*, vol. 8, no. 12, pp. 9865–9877, Aug. 2020.

[13] A. A. Khuwaja, Y. Chen, N. Zhao, M.-S. Alouini, and P. Dobbins, "A Survey of Channel Modeling for UAV Communications," *IEEE Commun. Surv. & Tutor.*, vol. 20, no. 4, pp. 2804–2821, July 2018.

[14] W. Khawaja, I. Guvenc, D. W. Matolak, U.-C. Fiebig, and N. Schneckenburger, "A Survey of Air-to-Ground Propagation Channel Modeling for Unmanned Aerial Vehicles," *IEEE Commun. Surv. & Tutor.*, vol. 21, no. 3, pp. 2361–2391, May 2019.

[15] D. W. Matolak, "Air-Ground Channels & Models: Comprehensive Review and Considerations for Unmanned Aircraft Systems," in *Proc. IEEE Aerospace Conference*, Big Sky, Mar. 2012, pp. 1–17.

[16] D. W. Matolak, and Ruoyu Sun, "Unmanned Aircraft Systems: Air-Ground Channel Characterization for Future Applications," *IEEE Veh. Technol. Mag.*, vol. 10, no. 2, pp. 79–85, Jun. 2015.

[17] C. Yan, L. Fu, J. Zhang, and J. Wang, "A Comprehensive Survey on UAV Communication Channel Modeling," *IEEE Access*, vol. 7, pp. 107769–107792, Aug. 2019.

[18] X. Cheng, Y. Li, and L. Bai, "UAV Communication Channel Measurement, Modeling, and Application," *J. Commun. Inf. Netw.*, vol. 4, no. 4, pp. 32–43, Dec. 2019.

[19] A. Ahmad, A. A. Cheema, and D. Finlay, "A Survey of Radio Propagation Channel Modelling for Low Altitude Flying Base Stations," *Computer Networks*, vol. 171, pp. 107122, Apr. 2020.

[20] L. Nasraoui, "Channel Modeling for UAV-Enabled Cellular Networks: A Survey," *IJRASET*, vol. 8, no. 5, pp. 2834–2841, May 2020.

[21] J. R. Child, "Air-to-Ground Propagation at 900 MHz," in *Proc. VTC'85*, 1985, pp. 73–80.

[22] W. Vergara, J. Levatich, and T. Carroll, "VHF Air-Ground Propagation Far Beyond the Horizon and Tropospheric Stability," *IEEE Trans. Antennas Propag.*, vol. 10, no. 5, pp. 608–621, Sept. 1962.

[23] M. Holzbock, and C. Senninger, "An Aeronautical Multimedia Service Demonstration at High Frequencies," *IEEE MultiMedia.*, vol. 6, no. 4, pp. 20–29, Oct. 1999.

[24] M. Rice, R. Dye, and K. Welling, "Narrowband Channel Model for Aeronautical Telemetry," *IEEE Trans. Aerosp. Electron. Syst.*, vol. 36, no. 4, pp. 1371–1376, Oct. 2000.

[25] M. Rice, A. Davis, and C. Bettweiser, "Wideband Channel Model for Aeronautical Telemetry," *IEEE Trans. Aerosp. Electron. Syst.*, vol. 40, no. 1, pp. 57–69, Jan. 2004.

[26] M. Rice, and M. Jensen, "Multipath Propagation for Helicopter-to-Ground MIMO Links," in *Proc. MLICOM'11*, Baltimore, MD, USA, Nov. 2011, pp. 447–452.

[27] M. Rice, and M. Saquib, "MIMO Equalization for Helicopter-to-Ground Communications," in *Proc. MLICOM'11*, Baltimore, MD, USA, Nov. 2011, pp. 501–506.

[28] Y. S. Meng, and Y. H. Lee, "Measurements and Characterizations of Air-to-Ground Channel Over Sea Surface at C-Band With Low Airborne Altitudes," *IEEE Trans. Veh. Technol.*, vol. 60, no. 4, pp. 1943–1948, May 2011.

[29] J. Kunisch, I. de la Torre, A. Winkelmann, M. Eube, and T. Fuss, "Wideband Time-Variant Air-to-Ground Radio Channel Measurements at 5 GHz," in *Proc. EuCAP'11*, 2011, pp. 1386–1390.

[30] J. Chen, B. Daneshrad, and Weijun Zhu, "MIMO Performance Evaluation for Airborne Wireless Communication Systems," in *Proc. MLICOM'11*, Baltimore, MD, USA, Nov. 2011, pp. 1827–1832.

[31] Y. S. Meng, and Y. H. Lee, "Study of Shadowing Effect by Aircraft Maneuvering for Air-to-Ground Communication." *Int. J. Electron. Commun.*, vol. 66, no. 1, pp. 7–11, Jan. 2012.

[32] K. Takizawa, F. Ono, H. Tsuji, and R. Miura, "Air-to-Air Radio Channel Measurement at 2.3 GHz for Unmanned Aircraft Services," in *Proc. WPMC'13*, Atlantic City, NJ, USA, June 2013, pp. 1–5.

[33] D. W. Matolak, and R. Sun, "Air-Ground Channel Measurements & Modeling for UAS," *IEEE Aerosp. Electron. Syst. Mag.*, vol. 29, no. 11, pp. 30–35, Nov. 2014.

[34] K. Takizawa, T. Kagawa, S. Lin, F. Ono, H. Tsuji, and R. Miura, "C-Band Aircraft-to-Ground (A2G) Radio Channel Measurement for Unmanned Aircraft Systems," in *Proc. WPMC'14*, Sydney, NSW, Australia, Sept. 2014, pp. 754–758.

[35] D. W. Matolak, and R. Sun, "Antenna and Frequency Diversity in the Unmanned Aircraft Systems Bands for the Over-Sea Setting," in *Proc. DASC'14*, Colorado Springs, CO, USA, Oct. 2014, pp. 6A4-1–6A4-10.

[36] R. Sun, and D. W. Matolak, "Over-Harbor Channel Modeling with Directional Ground Station Antennas for the Air-Ground Channel," in *Proc. MILCOM'14*, Baltimore, MD, USA, Oct. 2014, pp. 382–387.

[37] D. W. Matolak, and R. Sun, "Air-Ground Channel Characterization for Unmanned Aircraft Systems: The Hilly Suburban Environment," in *Proc. VTC'14*, Vancouver, BC, Canada, Sept. 2014, pp. 1–5.

[38] D. W. Matolak, and R. Sun, "Air-Ground Channel Characterization for Unmanned Aircraft Systems: The Over-Freshwater Setting," in *Proc. ICNS'14*, Herndon, VA, USA, Apr. 2014, pp. K1-1–K1-9.

[39] D. W. Matolak, and R. Sun, "Initial Results for Air-Ground Channel Measurements & Modeling for Unmanned Aircraft Systems: Over-Sea," in *Proc. AERO'14*, Big Sky, MT, USA, Mar. 2014, pp. 1–15.

[40] D. Matolak, and R. Sun, "Air-Ground Channel Measurements and Modeling for UAS," *IEEE Aerosp. Electron. Syst. Mag.*, vol. 29, no. 11, pp. 30–35, Nov. 2014.

[41] Y. Jiang, A. Tiwari, M. Rachid, and B. Daneshrad, "MIMO for Airborne Communications [Industry Perspectives]," *IEEE Wirel. Commun.*, vol. 21, no. 5, pp. 4–6, Oct. 2014.

[42] D. W. Matolak, and R. Sun, "Air–Ground Channel Characterization for Unmanned Aircraft Systems—Part I: Methods, Measurements, and Models for Over-Water Settings," *IEEE Trans. Veh. Technol.*, vol. 66, no. 1, pp. 26–44, Jan. 2017.

[43] D. W. Matolak, and R. Sun, "Air-Ground Channel Characterization for Unmanned Aircraft Aystems: The Near-Urban Environment," in *Proc. MILCOM'15*, Tampa, FL, USA, OCt. 2015, pp. 1656–1660.

[44] D. W. Matolak, and R. Sun, "Air-Ground Channels for UAS: Summary of Measurements and Models for L- and C-bands," in *Proc. ICNS'16*, Herndon, VA, USA, Apr. 2016, pp. 8B2-1–8B2-11.

[45] R. Sun, and D. W. Matolak, "Air–Ground Channel Characterization for Unmanned Aircraft Systems Part II: Hilly and Mountainous Settings," *IEEE Trans. Veh. Technol.*, vol. 66, no. 3, pp. 1913–1925, Mar. 2017.

[46] N. Schneckenburger, T. Jost, D. Shutin, et al., "Measurement of the L-Band Air-to-Ground Channel for Positioning Applications," *IEEE Trans. Aerosp. Electron. Syst.*, vol. 52, no. 5, pp. 2281–2297, Oct. 2016.

[47] D. W. Matolak, and R. Sun, "Air–Ground Channel Characterization for Unmanned Aircraft Systems—Part III: The Suburban and Near-Urban Environments," *IEEE Trans. Veh. Technol.*, vol. 66, no. 8, pp. 6607–6618, Aug. 2017.

[48] J. Kim, and I. Lee, "Channel Measurements and Characterizations for Long Range Air-to-Ground Communication Systems in the UHF Band," *IEEE Access*, vol. 10, pp. 101880–101888, 2022.

[49] M. Simunek, P. Pechac, and F. P. Fontán, "Feasibility of UAV Link Space Diversity in Wooded Areas," *Int. J. Antennas Propag.*, vol. 2013, June 2013.

[50] M. Simunek, F. P. Fontán, and P. Pechac, "The UAV Low Elevation Propagation Channel in Urban Areas: Statistical Analysis and Time-Series Generator," *IEEE Trans. Antennas Propag.*, vol. 61, no. 7, pp. 3850–3858, July. 2013.

[51] T. Tavares, P. Sebastião, N. Souto, F. J. Velez, F. Cercas, et al., "Generalized LUI Propagation Model for UAVs Communications Using Terrestrial Cellular Networks," in *Proc. VTC'15*, Boston, MA, USA, Sept. 2015, pp. 1–6.

[52] M. Kvicera, F. Pérez Fontán, J. Israel, and P. Pechac, "A New Model for Scattering From Tree Canopies Based on Physical Optics and Multiple Scattering Theory," *IEEE Trans. Antennas Propag.*, vol. 65, no. 4, pp. 1925–1933, Apr. 2017.

[53] V. Nikolaidis, N. Moraitis, and A. G. Kanatas, "Dual-Polarized Narrowband MIMO LMS Channel Measurements in Urban Environments," *IEEE Trans. Antennas Propag.*, vol. 65, no. 2, pp. 763–774, Feb. 2017.

[54] X. Cai, T. Izydorczyk, J. Rodríguez-Piñeiro, I. Z. Kovács, J. Wigard, et al., "Empirical Low-Altitude Air-to-Ground Spatial Channel Characterization for Cellular Networks Connectivity," *IEEE J. Select. Areas Commun.*, vol. 39, no. 10, pp. 2975–2991, Oct. 2021.

[55] Y. Zhou, X. Huang, D. Zhang, B. Li, J. Zeng, et al., "5G-Based Measurements and Characterizations of Low-Altitude Tethered Balloon Multipath Channel," in *Proc. VTC'21*, Helsinki, Finland, Apr. 2021, pp. 1–5.

[56] T. Brown, B. Argrow, C. Dixon, S. Doshi, R.-G. Thekkekunnel, et al., "Ad Hoc UAV Ground Network (AUGNet)," in *Proc. AIAA'04*, Chicago, USA, Sep. 2004.

[57] C.-M. Cheng, P.-H. Hsiao, H.-T. Kung, and D. Vlah, "Performance Measurement of 802.11a Wireless Links from UAV to Ground Nodes with Various Antenna Orientations," in *Proc. ICCCN'06*, Arlington, VA, USA, Oct. 2006, pp. 303–308.

[58] J. Allred, A. Hasan, S. Panichsakul, W. Pisano, P. Gray, et al., "SensorFlock: An Airborne Wireless Sensor Network of Micro-air Vehicles." in *Proc. SenSys'07*, Sydney, NSW, Australia, Nov. 2007, pp.117–129.

[59] Lee, Yee Hui, Yu Song Meng, and Yew Heng Heng. "Experimental Characterizations of An Air to Land Channel Over Sea Surface in C Band." in *Proc. XXIXth URSI General Assembly*, 2008.

[60] H. D. Tu, and S. Shimamoto, "A Proposal of Wide-Band Air-to-Ground Communication at Airports Employing 5-GHz Band," in *Proc. WCNC'09*, Budapest, Hungary, Apr. 2009, pp. 1–6.

[61] M. Walter, S. Gligorević, T. Detert, and M. Schnell, "UHF/VHF Air-to-Air Propagation Measurements," in *Proc. EuCAP'10*, Barcelona, Spain, Apr. 2010, pp. 1–5.

[62] J. Romeu, A. Aguasca, J. Alonso, S. Blanch, and R. R. Martins, "Small UAV Radiocommunication Channel Characterization," in *Proc. EuCAP'10*, Barcelona, Spain, Apr. 2010, pp. 1–5.

[63] N. Goddemeier, K. Daniel, and C. Wietfeld, "Coverage Evaluation of Wireless Networks for Unmanned Aerial Systems," in *Proc. GC Wkshps'10*, Miami, FL, USA, Dec. 2010, pp. 1760–1765.

[64] H. T. Kung, C. -K. Lin, T. -H. Lin, S. J. Tarsa, and D. Vlah, "Measuring Diversity on a Low-Altitude UAV in a Ground-to-Air Wireless 802.11 Mesh Network," in *Proc. GC Wkshps'10*, Miami, FL, USA, Dec. 2010, pp. 1799–1804.

[65] T. J. Willink, C. C. Squires, G. W. K. Colman, and M. T. Muccio, "Measurement and Characterization of Low-Altitude Air-to-Ground MIMO Channels," *IEEE Trans. Veh. Technol.*, vol. 65, no. 4, pp. 2637–2648, Apr. 2016.

[66] F. Ono, T. Kagawa, H. Tsuji, R. Miura, and F. Kojima, "Measurements on C-Band Air-to-Air Channel for Coexistence Among Multiple Unmanned Aircraft Systems,"in *Proc. ICUAS'17*, Miami, FL, USA, June 2017, pp. 1160–1164.

[67] H. An, K. Guan, W. Li, J. Zhang, D. He, et al., "Measurement and Ray-tracing for UAV Air-to-air Channel Modeling," in *Proc. ICEICT'22*, Hefei, China, Aug. 2022, pp. 415–420.

[68] E. Yanmaz, R. Kuschnig, and C. Bettstetter, "Channel Measurements Over 802.11a-Based UAV-to-Ground Links," in *Proc. GC Wkshps'11*, Houston, TX, USA, Dec.2011, pp. 1280–1284.

[69] E. Yanmaz, R. Kuschnig, and C. Bettstetter, "Achieving Air-Ground Communications in 802.11 Networks with Three-Dimensional Aerial Mobility," in *Proc. INFOCOM'13*, Turin, Italy, Apr. 2013, pp. 120–124.

[70] E. Yanmaz, S. Hayat, J. Scherer, and C. Bettstetter, "Experimental Performance Analysis of Two-Hop Aerial 802.11 Networks," in *Proc. WCNC'14*, Istanbul, Turkey, Apr. 2014, pp. 3118–3123.

[71] S. Hayat, E. Yanmaz, and C. Bettstetter, "Experimental Analysis of Multipoint-to-Point UAV Communications with IEEE 802.11n and 802.11ac," in *Proc. PIMRC'15*, Hong Kong, China, Aug. 2015, pp. 1991–1996.

[72] N. Goddemeier, and C. Wietfeld, "Investigation of Air-to-Air Channel Characteristics and a UAV Specific Extension to the Rice Model," in *Proc. GC Wkshps'15*, San Diego, CA, USA, Dec. 2015, pp. 1–5.

[73] L. Afonso, N. Souto, P. Sebastiao, M. Ribeiro, T. Tavares, et al., "Cellular for the Skies: Exploiting Mobile Network Infrastructure for Low Altitude Air-to-Ground Communications," *IEEE Trans. Aerosp. Electron. Syst.*, vol. 31, no. 8, pp. 4–11, Aug. 2016.

[74] W. Khawaja, I. Guvenc, and D. Matolak, "UWB Channel Sounding and Modeling for UAV Air-to-Ground Propagation Channels," in *Proc. GLOBECOM'16*, Washington, DC, USA, Dec. 2016, pp. 1–7.

[75] N. Ahmed, S. S. Kanhere, and S. Jha, "Utilizing Link Characterization for Improving the Performance of Aerial Wireless Sensor Networks," *IEEE J. Select. Areas Commun.*, vol. 31, no. 8, pp. 1639–1649, Aug. 2013.

[76] R. M. Gutierrez, H. Yu, Y. Rong, and D. W. Bliss, "Time and Frequency Dispersion Characteristics of the UAS Wireless Channel in Residential and Mountainous Desert Terrains," in *Proc. CCNC'17*, Las Vegas, NV, USA, Jan. 2017, pp. 516–521.

[77] X. Cai, A. Gonzalez-Plaza, D. Alonso, L. Zhang, C. B. Rodriguez, et al., "Low Altitude UAV Propagation Channel Modelling," in *Proc. EUCAP'17*, Paris, France, Mar. 2017, pp. 1443–1447.

[78] X. Ye, X. Cai, X. Yin, J. Rodriguez-Pineiro, L. Tian, et al., "Air-to-Ground Big-Data-Assisted Channel Modeling Based on Passive Sounding in LTE Networks," in *Proc. GC Wkshps'17*, Singapore, Dec. 2017, pp. 1–6.

[79] E. Teng, J. D. Falcao, C. R. Dominguez, F. Mokaya, P. Zhang, et al., "Aerial Sensing and Characterization of Three-Dimensional RF Fields," *Data Process*, vol. 10, pp. 13–18, 2016.

[80] E. Teng, J. Diogo Falcão, and B. Iannucci, "Holes-in-the-Sky: A Field Study on Cellular-Connected UAS," in *Proc. ICUAS'17*, Miami, FL, USA, June 2017, pp. 1165–1174.

[81] H. Boeglen, A. Traore, M. M. Peinado, R. Lefort, and R. Vauzelle, "An SDR Based Channel Sounding Technique for Embedded Systems," in *Proc. EUCAP'17*, Paris, France, Mar. 2017, pp. 3286–3290

[82] R. Amorim, H. Nguyen, P. Mogensen, I. Z. Kovács, J. Wigard, et al., "Radio Channel Modeling for UAV Communication Over Cellular Networks," *IEEE Wireless Commun. Lett.*, vol. 6, no. 4, pp. 514–517, Aug. 2017.

[83] Z. Qiu, X. Chu, C. R. Cesar, et al., "Low Altitude UAV Air-to-Ground Channel Measurement and Modeling in Semiurban Environments," *Wirel. Commun. Mob. Comput.*, vol. 2017, pp. 1–11, Dec. 2017.

[84] K. Wang, R. Zhang, L. Wu, Z. Zhong, L. He, et al., "Path Loss Measurement and Modeling for Low-Altitude UAV Access Channels," in *Proc.VTC'17*, Toronto, ON, Canada, Sept. 2017, pp. 1–5.

[85] H. C. Nguyen, R. Amorim, J. Wigard, I. Z. Kovacs, and P. Mogensen, "Using LTE Networks for UAV Command and Control Link: A Rural-Area Coverage Analysis," in *Proc. VTC'17*, Toronto, ON, Canada, Sept. 2017, pp. 1–6.

[86] A. Al-Hourani, and K. Gomez, "Modeling Cellular-to-UAV Path-Loss for Suburban Environments," *IEEE Wirel. Commun. Lett.*, vol. 7, no. 1, pp. 82–85, Feb. 2018.

[87] Z. Cui, C. Briso, K. Guan, D. W. Matolak, C. Calvo-Ramirez, et al. "Low-Altitude UAV Air-Ground Propagation Channel Measurement and Analysis in a Suburban Environment at 3.9 GHz," *IET Microw. Antennas Propag.*, vol. 13, no. 9, pp. 1503–1508, July 2019.

[88] K. Tu, J. Rodríguez-Piñeiro, X. Yin, and L. Tian, "Low Altitude Air-to-Ground Channel Modelling Based on Measurements in a Suburban Environment," in *Proc. WCSP'19*, Xi'an, China, Dec 2019, pp. 1–6.

[89] X. Cai, J. Rodríguez-Piñeiro, X. Yin, N. Wang, B. Ai, et al., "An Empirical Air-to-Ground Channel Model Based on Passive Measurements in LTE," *IEEE Trans. Veh. Technol.*, vol. 68, no. 2, pp. 1140–1154, Feb. 2019.

[90] X. Cai, N. Wang, J. Rodríguez-Piñeiro, X. Yin, A. P. Yuste, et al., "Low Altitude Air-to-Ground Channel Characterization in LTE Network," in *Proc. EuCAP'19*, Krakow, Poland, Mar. 2019, pp. 1–5.

[91] A. E. Garcia, M. Ozger, A. Baltaci, S. Hofmann, D. Gera, et al., "Direct Air to Ground Communications for Flying Vehicles: Measurement and Scaling Study for 5G," in *Proc. 5GWF'19*, Dresden, Germany, Sept. 2019, pp. 310–315.

[92] Y. Wang, R. Zhang, B. Li, X. Tang, and D. Wang, "Angular Spread Analysis and Modeling of UAV Air-to-Ground Channels at 3.5 GHz," in *Proc. WCSP'19*, Xi'an, China, Oct. 2019, pp. 1–5.

[93] X. Cai, C. Zhang, J. Rodríguez-Piñeiro, X. Yin, W. Fan, et al., "Interference Modeling for Low-Height Air-to-Ground Channels in Live LTE Networks, *IEEE Antennas Wirel. Propag. Lett.*, vol. 18, no. 10, pp. 2011–2015, Oct. 2019.

[94] D. Becker, and L. Schalk, "Enabling Air-to-Air Wideband Channel Measurements between Small Unmanned Aerial Vehicles with Optical Fibers," in *Proc DASC'19*, San Diego, CA, USA, Sept. 2019, pp. 1–7.

[95] G. Zhang, X. Cai, W. Fan, and G. F. Pedersen, "A USRP-Based Channel Sounder for UAV Communications," in *Proc. EuCAP'20*, Copenhagen, Denmark, Mar. 2020, pp. 1—4.

[96] Z. Cui, C. Briso-Rodríguez, K. Guan, İ. Güvenç, and Z. Zhong, "Wideband Air-to-Ground Channel Characterization for Multiple Propagation Environments," *IEEE Antennas Wirel. Propag. Lett.*, vol. 19, no. 9, pp. 1634–1638, Sept. 2020.

[97] Z. Cui, C. Briso-Rodríguez, K. Guan and Z. Zhong, "Ultra-Wideband Air-to-Ground Channel Measurements and Modeling in Hilly Environment," in *Proc. ICC'20*, Dublin, Ireland, June 2020, pp. 1–6.

[98] Z. Cui, C. Briso-Rodríguez, K. Guan, Z. Zhong, and F. Quitin, "Multi-Frequency Air-to-Ground Channel Measurements and Analysis for UAV Communication Systems," *IEEE Access*, vol. 8, pp. 110565–110574, 2020.

[99] M. Polese, L. Bertizzolo, L. Bonati, A. Gosain, and T. Melodia, "An Experimental mmWave Channel Model for UAV-to-UAV Communications," in *Proc. ACM'20*, London, United Kingdom, Sep. 2020, pp. 1–6.

[100] J. Rodriguez-Pineiro, T. Dominguez-Bolano, X. Cai, Z. Huang, and X. Yin, "Air-to-Ground Channel Characterization for Low-Height UAVs in Realistic Network Deployments," *IEEE Trans. Antennas Propagat.*, vol. 69, no. 2, pp. 992–1006, Feb. 2021.

[101] W. Khawaja, O. Ozdemir, F. Erden, I. Guvenc, and D. W. Matolak, "Ultra-Wideband Air-to-Ground Propagation Channel Characterization in an Open Area," *IEEE Trans. Aerosp. Electron. Syst.*, vol. 56, no. 6, pp. 4533–4555, Dec. 2020.

[102] D. Becker, U. Fiebig, and L. Schalk, "Wideband Channel Measurements and First Findings for Low Altitude Drone-to-Drone Links in an Urban Scenario," in *Proc. EuCAP'20*, Copenhagen, Denmark, Mar. 2020, pp. 1–5.

[103] Z. Cui, K. Guan, C. Oestges, C. Briso-Rodríguez, B. Ai, et al., "Cluster-Based Characterization and Modeling for UAV Air-to-Ground Time-Varying Channels," *IEEE Trans. Veh. Technol.*, vol. 71, no. 7, pp. 6872–6883, Jul. 2022.

[104] B. Ning, T. Li, K. Mao, X. Chen, M. Wang, et al., "A UAV-Aided Channel Sounder for Air-to-Ground Channel Measurements," *Phys. Commun.*, vol. 47, pp. 101366, Aug. 2021.

[105] J. Gomez-Ponce, T. Choi, N. A. Abbasi, A. Adame, A. Alvarado, et al., "Air-to-Ground Directional Channel Sounder With Drone and 64-antenna Dual-polarized Cylindrical Array," in *Proc. ICC'21*, Montreal, Canada, Jun. 2021, pp. 1–6.

[106] B. Ning, K. Mao, M. Wang, H. Li, X. Chen, et al., "Machine Learning Based Angle Estimation for Air-to-Ground Channel Measurements," in *Proc. WCSP'21*, Changsha, China, Oct. 2021, pp. 1–5.

[107] N. C. Matson, S. M. Hashir, S. Song, D. Rajan, and J. Camp, "Effect of Antenna Orientation on the Air-to-Air Channel in Arbitrary 3D Space," in *Proc. WoWMoM'21*, Pisa, Italy, June 2021, pp. 298–303.

[108] B. Ede, B. Kaplan, İ. Kahraman, S. Kesir, S. Yarkan, et al., "Measurement-Based Large Scale Statistical Modeling of Air-to-Air Wireless UAV Channels via Novel Time-Frequency Analysis," *IEEE Wirel. Commun. Lett.*, vol. 11, no. 1, pp. 136–140, Jan. 2022.

[109] V. Semkin, E. M. Vitucci, F. Fuschini, M. Barbiroli, V. Degli-Esposti, et al., "Characterizing the UAV-to-Machine UWB Radio Channel in Smart Factories," *IEEE Access*, vol. 9, pp. 76542–76550, 2021.

[110] V. Semkin, S. Kang, J. Haarla, W. Xia, I. Huhtinen, et al., "Lightweight UAV-based Measurement System for Air-to-Ground Channels at 28 GHz," in *Proc. PIMRC'21*, Helsinki, Finland, Sept. 2021, pp. 848–853.

[111] V. Semkin, and I. Huhtinen, "Millimeter-wave UAV-based Channel Measurement Setup," in *Proc. VTC'21*, Helsinki, Finland, Apr. 2021, pp. 1–2.

[112] F. Fuschini, M. Barbiroli, E. M. Vitucci, V. Semkin, C. Oestges, et al., "An UAV-Based Experimental Setup for Propagation Characterization in Urban Environment," *IEEE Trans. Instrum. Meas.*, vol. 70, pp. 1–11, Aug. 2021.

[113] L. Val-Terrón, J. J. Escudero-Garzás, L. Pérez-Roca, A. M. Vega-Viejo, and Á. Alves-González, "Air-to-Ground Channel Characterization for Unmanned Aerial Vehicles Based on Field Measurements in 5G at 3.5 GHz," in *Proc. WiMob'22*, Thessaloniki, Greece, Oct. 2022, pp. 453–456.

[114] Y. Lv, Y. Wang, J. Chai, and W. Wang, "Ultra Wideband Channel Measurement and Analysis for Low Altitude UAV Air-to-Ground Scenario," in *Proc. ISAPE'21*, Zhuhai, China, Dec. 2021, pp. 1–3.

[115] M. Badi, D. Rajan, and J. Camp, "Measurement-Based Characterization of Human Body Impact on Ultra-low UAV-to-Ground Channels," in *Proc. MILCOM'21*, San Diego, CA, USA, Dec. 2021, pp. 556–561.

[116] C. Yu, Y. Liu, H. Chang, J. Zhang, M. Zhang, et al., "AG Channel Measurements and Characteristics Analysis in Hilly Scenarios for 6G UAV Communications," *China Commun.*, vol. 19, no. 11, pp. 32–46, Nov. 2022.

[117] B. Ede, B. Kaplan, İ. Kahraman, S. Kesir, S. Yarkan, et al., "Measurement-Based Large Scale Statistical Modeling of Air–to–Air Wireless UAV Channels via Novel Time–Frequency Analysis," *IEEE Wirel. Commun. Lett.*, vol. 11, no. 1, pp. 136–140, Jan. 2022.

[118] T. Choi, J. Gomez-Ponce, C. Bullard, I. Kanno, M. Ito, et al., "Using a Drone Sounder to Measure Channels for Cell-Free Massive MIMO Systems," in *Proc. WCNC'22*, Austin, TX, USA, Apr. 2022, pp. 2506–2511.

[119] K. Mao, Q. Zhu, F. Duan, Y. Qiu, M. Song, et al., "A2G Channel Measurement and Characterization via TNN for UAV Multi-Scenario Communications," in *Proc. GLOBECOM'22*, Rio de Janeiro, Brazil, Dec. 2022, pp. 4461–4466.

[120] H. Li, X. Chen, K. Mao, Q. Zhu, Y. Qiu, et al., "Air-to-Ground Path Loss Prediction Using Ray Tracing and Measurement Data Jointly Driven DNN," *Comput. Commun.*, vol. 196, pp. 268—276, Dec. 2022.

[121] H. Li, X. Chen, K. Mao, F. Duan, Y. Qiu, et al., "Sparse Measurement Data Driven Air-to-Ground Path Loss Prediction over Vegetation Area," in *Proc. VTC'22*, London/Beijing, Sep. 2022, pp. 1—5.

[122] S. G. Sanchez, S. Mohanti, D. Jaisinghani, and K. R. Chowdhury, "Millimeter-Wave Base Stations in the Sky: An Experimental Study of UAV-to-Ground Communications," *IEEE Trans. Mob. Comput.*, vol. 21, no. 2, pp. 644–662, Feb. 2022.

[123] K. Mao, Q. Zhu, Y. Qiu, X. Liu, M. Song, et al., "A UAV-Aided Real-Time Channel Sounder for Highly Dynamic Nonstationary A2G Scenarios," *IEEE Trans. Instrum. Meas.*, vol. 72, pp. 1–15, Aug. 2023.

[124] Z. Ma, B. Ai, R. He, G. Wang, Y. Niu, et al., "Impact of UAV Rotation on MIMO Channel Characterization for Air-to-Ground Communication Systems," *IEEE Trans. Veh. Technol.*, vol. 69, no. 11, pp. 12418–12431, Nov. 2020.

[125] M. A. Jasim, H. Shakhatreh, N. Siasi, A. H. Sawalmeh, A. Aldalbahi, et al., "A Survey on Spectrum Management for Unmanned Aerial Vehicles (UAVs)," *IEEE Access*, vol. 10, pp. 11443–11499, Dec. 2022.

[126] R. J. Kerczewski, J. D. Wilson, and W. D. Bishop, "UAS CNPC satellite link performance — Sharing spectrum with terrestrial systems," in Proc. *IEEE Aerosp. Conf.*, Big Sky, MT, USA, Mar. 2016, pp. 1–9.

[127] J. Lee, E. Tejedor, K. Ranta-aho, H. Wang, K. T. Lee, et al., "Spectrum for 5G: Global Status, Challenges, and Enabling Technologies," *IEEE Commun. Mag.*, vol. 56, no. 3, pp. 12–18, Mar. 2018.

[128] A. F. Molisch, "Ultrawideband Propagation Channels-Theory, Measurement, and Modeling," *IEEE Trans. Veh. Technol.*, vol. 54, no. 5, pp. 1528–1545, Sept. 2005.

[129] Y. Tan, C.-X. Wang, J. Ødum Nielsen, G. F. Pedersen, Q. Zhu, et al., "A Novel B5G Frequency Nonstationary Wireless Channel Model," *IEEE Trans. Antennas Propagat.*, vol. 69, no. 8, pp. 4846–4860, Feb. 2021.

[130] V. Kristem, C. U. Bas, R. Wang, and A. F. Molisch, "Outdoor Wideband Channel Measurements and Modeling in the 3–18 GHz Band," *IEEE Trans. Wirel. Commun.*, vol. 17, no. 7, pp. 4620–4633, Apr. 2018.

[131] K. Mao, Q. Zhu, R. Feng, F. Duan, Y. Miao, et al., "UWB Channel Modeling and Simulation with Continuous Frequency Response," *China Commun.*, vol. 19, no. 11, pp. 88–98, Nov. 2022.

[132] F. Zhang, and W. Fan, "Near-Field Ultra-Wideband mmWave Channel Characterization Using Successive Cancellation Beamspace UCA Algorithm," *IEEE Trans. Veh. Technol.*, vol. 68, no. 8, pp. 7248–7259, July 2019.

[133] M. Z. M. Hamdalla, A. N. Caruso, and A. M. Hassan, "Electromagnetic Compatibility Analysis of Quadcopter UAVs Using the Equivalent Circuit Approach," *IEEE Open J. Antennas Propag.*, vol. 3, pp. 1090–1101, Sept. 2022.

[134] R. Cesoni, G. Fantin, G. Spadini, F. Tonelli, T. Sun, et al., "Experimental Tests on Electromagnetic Compatibility of a UAV in the Proximity of High Voltage Power Lines," in *Proc. ICOLIM'22*, Turin, Italy, June 2022, pp. 1–5.

[135] M. Höyhtyä, A. Mämmelä, M. Eskola, et al., "Spectrum Occupancy Measurements: A Survey and Use of Interference Maps," *IEEE Commun. Surv. & Tutor.*, vol. 18, no. 4, pp. 2386–2414, Apr. 2016.

[136] Q. Song, Y. Zeng, J. Xu, and S. Jin, "A Survey of Prototype and Experiment for UAV Communications," *Sci. China Inf. Sci.*, vol. 64, no. 4, pp. 140301, Feb. 2021.

[137] W. Mei, and R. Zhang, "Aerial-Ground Interference Mitigation for Cellular-Connected UAV," *IEEE Wirel. Commun.*, vol. 28, no. 1, pp. 167–173, Feb. 2021.

[138] RUSK MIMO channel sounder, "https://www.tu-ilmenau.de/universitaet/fakultaeten/fakultaet-elektrotechnik-und-informationstechnik/profil/institute-und-fachgebiete/fachgebiet-nachrichtentechnik/mscsp/mscsp-labs/mimo-rusk-channel-sounder."

[139] Elektrobit PropSound sounder, "https://www.hamfu.ch/_upload/Multidimensional_Channel_Sounding_-_Instruments_Methods_Results.pdf."

[140] Keysight 5G channel sounder, "https://www.keysight.com/nl/en/assets/7018-05100/configuration-guides/5992-1326.pdf."

[141] T. Zhou, B. Hua, Q. Zhu, H. Ni, K. Mao, et al., "Spatial-temporal Correlations of U2V Channel Considering Fuselage Posture and Antenna Pattern," in *Proc. EuCAP'22*, Madrid, Spain, Mar. 2022, pp. 1–5.

[142] F. Erden, O. Ozdemir, W. Khawaja, and I. Guvenc, "Correction of Channel Sounding Clock Drift and Antenna Rotation Effects for mmWave Angular Profile Measurements," *IEEE Open J. Antennas Propag.*, vol. 1, pp. 71–87, Mar. 2020.

[143] P. Zhang, H. Wang, and W. Hong, "Radio Propagation Measurement and Cluster-Based Analysis for Millimeter-Wave Cellular Systems in Dense Urban Environments," *Front. Inf. Technol. & Electron. Eng.*, vol. 22, no. 4, pp. 471–487, Apr. 2021.

[144] M. Li, F. Zhang, Y. Ji, and W. Fan, "Virtual Antenna Array With Directional Antennas for Millimeter-Wave Channel Characterization," *IEEE Trans. Antennas Propag.*, vol. 70, no. 8, pp. 6992–7003, Aug. 2022.

[145] Z. Guan, and T. Kulkarni, "On the Effects of Mobility Uncertainties on Wireless Communications Between Flying Drones in the mmWave/THz Bands," in *Proc. INFOCOM'19*, Paris, France, Apr. 2019, pp. 768–773.

[146] R. Wu, X. Zhao, Y. Liu, and Y. Song, "Initial Pointing Technology of Line of Sight and Its Experimental Testing in Dynamic Laser Communication System," *IEEE Photon. J.*, vol. 11, no. 2, pp. 1–8, Apr. 2019.

[147] M. Banagar, H. S. Dhillon, and A. F. Molisch, "Impact of UAV Wobbling on the Air-to-Ground Wireless Channel," *IEEE Trans. Veh. Technol.*, vol. 69, no. 11, pp. 14025–14030, Nov. 2020.

[148] S. Yang, Z. Zhang, J. Zhang, and J. Zhang, "Impact of Rotary-Wing UAV Wobbling on Millimeter-Wave Air-to-Ground Wireless Channel," *IEEE Trans. Veh. Technol.*, vol. 71, no. 9, pp. 9174–9185, Sept. 2022.

[149] H. Shen, Q. Wang, S. Gao, and H. Yu, "Impact of UAV Wobbling on the Air-to-Terrestrial Wireless Communication Channels in Various Frequency Bands," in *Proc. ICSPS'22*, Jiangsu, China, 2022, pp. 667–673.

[150] A. Kaadan, H. H. Refai, and P. G. Lopresti, "Multielement FSO Transceivers Alignment for Inter-UAV Communications," *J. Lightw. Technol.*, vol. 32, no. 24, pp. 4785–4795, Dec. 2014.

[151] J. Bian, C. -X. Wang, Y. Liu, J. Tian, J. Qiao, et al., "3D Non-Stationary Wideband UAV-to-Ground MIMO Channel Models Based on Aeronautic Random Mobility Model," *IEEE Trans. Veh. Technol.*, vol. 70, no. 11, pp. 11154–11168, Nov. 2021.

[152] A. Venon, Y. Dupuis, P. Vasseur, and P. Merriaux, "Millimeter Wave FMCW RADARs for Perception, Recognition and Localization in Automotive Applications: A Survey," *IEEE Trans. Intell. Veh.*, vol. 7, no. 3, pp. 533–555, Sept. 2022.

[153] H.-J. Zepernick, and A. Finger, "Pseudo Random Signal Processing: Theory and Application," *John Wiley & Sons*, July 2013.

[154] D. Zhang, B. Ai, D. Fei, and Z. Chen. "Comparison of Different Sounding Waveforms for a Wideband Correlation Channel Sounder," in *Proc. EITRT'21*, Singapore, 2021, pp. 119–126.

[155] M. M. Silva, L. d. S. Mello, C. V. Rodríguez R., and P. G. Castellanos, "Wideband Channel Sounding Using Modulated OFDM Signals," in *Proc. APWC'18*, Cartagena, Colombia, Sept. 2018, pp. 1–4.

[156] F. Burmeister, R. Jacob, A. Traßl, N. Schwarzenberg, and G. Fettweis, "Dealing with Fractional Sampling Time Offsets for Unsynchronized Mobile Channel Measurements," *IEEE Wirel. Commun. Lett.*, vol. 10, no. 12, pp. 2781–2785, Dec. 2021.

[157] O. Seijo, I. Val, and J. A. Lopez-Fernandez, "Portable Full Channel Sounder for Industrial Wireless Applications With Mobility by Using Sub-Nanosecond Wireless Time Synchronization," *IEEE Access*, vol. 8, pp. 175576–175588, 2020.

[158] X. Cai, M. Zhu, A. Fedorov, F. Tufvesson, "Enhanced Effective Aperture Distribution Function for Characterizing Large-Scale Antenna Arrays," *arXiv*, 2023.

[159] Z. Bodnar, Z. Herczku, and I. Frigyes, "Noise Threshold Dependency of the RMS Delay Spread in Wideband Measurements of Radio Propagation Channels," in *Proc. ITS'98*, 1998, pp. 312–317.

[160] J. Gomez-Ponce, N. A. Abbasi, Z. Cheng, S. Abu-Surra, G. Xu, et al., "Impact of Noisy Measurements with Fourier-Based Evaluation on Condensed Channel Parameters." *IEEE Trans. Wirel. Commun.*, early access, Dec. 2023.

[161] C.-X. Wang, Z. Lv, Y. Chen, and H. Haas, "A Complete Study of Space-Time-Frequency Statistical Properties of the 6G Pervasive Channel Model," *IEEE Trans. Commun.*, early access, 2023, doi: 10.1109/TCOMM.2023.3307144.

[162] C.-X. Wang, Z. Lv, X. Gao, X.-H. You, Y. Hao, et al., "Pervasive Wireless Channel Modeling Theory and Applications to 6G GBSMs for All Frequency Bands and All Scenarios," *IEEE Trans. Veh. Technol.*, vol. 71, no. 9, pp. 9159–9173, Sept. 2022.

[163] X. Cai, X. Cheng, and F. Tufvesson, "Toward 6G with Terahertz Communications: Understanding the Propagation Channels," *IEEE Commun. Mag.*, arXiv, 2023.

[164] Z. Xiao, L. Zhu, Y. Liu, P. Yi, R. Zhang, et al., "A Survey on Millimeter-Wave Beamforming Enabled UAV Communications and Networking," *IEEE Communications Surveys & Tutorials*, vol. 24, no. 1, pp. 557–610, Firstquarter 2022.

[165] A. C. Pogaku, D. -T. Do, B. M. Lee, and N. D. Nguyen, "UAV-Assisted RIS for Future Wireless Communications: A Survey on Optimization and Performance Analysis," *IEEE Access*, vol. 10, pp. 16320–16336, Feb. 2022.

[166] C.-X. Wang, X. You, X. Gao, X. Zhu, Z. Li, et al., "On the Road to 6G: Visions, Requirements, Key Technologies and Testbeds," *IEEE Commun. Surveys Tuts.*, vol. 25, no. 2, pp. 905–974, 2nd Quart. 2023.

[167] C.-X. Wang, J. Huang, H. Wang, X. Gao, X.-H. You, et al., "6G Wireless Channel Measurements and Models: Trends and Challenges," *IEEE Veh. Technol. Mag.*, vol. 15, no. 4, pp. 22–32, Dec. 2020.

[168] B. Xiong, Z. Zhang, H. Jiang, J. Zhang, L. Wu, et al., "A 3D Non-Stationary MIMO Channel Model for Reconfigurable Intelligent Surface Auxiliary UAV-to-Ground mmWave Communications," *IEEE Trans. Wirel. Commun.*, vol. 21, no. 7, pp. 5658–5672, July 2022.

[169] A. -A. A. Boulogeorgos, A. Alexiou, and M. D. Renzo, "Outage Performance Analysis of RIS-Assisted UAV Wireless Systems Under Disorientation and Misalignment," *IEEE Trans. Veh. Technol.*, vol. 71, no. 10, pp. 10712–10728, Oct. 2022.

[170] X.-H. You, C.-X. Wang, J. Huang, X. Gao, Z. Zhang, et al., "Towards 6G Wireless Communication Networks: Vision, Enabling Technologies, and New Paradigm Shifts," *Sci. China Inf. Sci.*, vol. 64, no. 1, Jan. 2021.

[171] G. Lee, W. Saad, and M. Bennis, "Online Optimization for UAV-Assisted Distributed Fog Computing in Smart Factories of Industry 4.0," in *Proc. GLOBECOM'18*, Abu Dhabi, United Arab Emirates, Dec. 2018, pp. 1–6.